Bioorganic & Medicinal Chemistry 25 (2017) 1202–1218

Contents lists available at ScienceDirect

Bioorganic & Medicinal Chemistry

journal homepage: www.elsevier.com/locate/bmc

Bifunctional conjugates with potent inhibitory activity towards cyclooxygenase and histone deacetylase

Idris Raji [a], Fatima Yadudu [a], Emily Janeira [e], Shaghayegh Fathi [a], Lindsey Szymczak [c], James Richard Kornacki [c], Kensei Komatsu [d], Jian-Dong Li [d], Milan Mrksich [c], Adegboyega K. Oyelere [a,b,*]

[a] School of Chemistry and Biochemistry, Georgia Institute of Technology, Atlanta, GA 30332-0400, USA
[b] Parker H. Petit Institute for Bioengineering and Bioscience, Georgia Institute of Technology, Atlanta, GA 30332-0400, USA
[c] Departments of Chemistry and Biomedical Engineering, Northwestern University, 2145 Sheridan Road, Evanston, IL 60208-3113, USA
[d] Center for Inflammation, Immunity & Infection, Institute for Biomedical Sciences, Georgia State University, USA
[e] Department of Chemistry, University of North Carolina at Chapel Hill, Chapel Hill, NC 27514, USA

ARTICLE INFO

Article history:
Received 4 November 2016
Revised 17 December 2016
Accepted 20 December 2016
Available online 24 December 2016

ABSTRACT

We herein disclose a series of compounds with potent inhibitory activities towards histone deacetylases (HDAC) and cyclooxygenases (COX). These compounds potently inhibited the growth of cancer cell lines consistent with their anti-COX and anti-HDAC activities. While compound **2b** showed comparable level of COX-2 selectivity as celecoxib, compound **11b** outperformed indomethacin in terms of selectivity towards COX-2 relative to COX-1. An important observation with our lead compounds (**2b**, **8**, **11b**, and **17b**) is their enhanced cytotoxicity towards androgen dependent prostate cancer cell line (LNCaP) relative to androgen independent prostate cancer cell line (DU-145). Interestingly, compounds **2b** and **17b** arrested the cell cycle progression of LNCaP in the S-phase, while compound **8** showed a G0/G1 arrest, similar to SAHA. Relative to SAHA, these compounds displayed tumor-selective cytotoxicity as they have low anti-proliferative activity towards healthy cells (VERO); an attribute that makes them attractive candidates for drug development.

1. Introduction

Aberrant epigenetic regulation and inflammation play significant roles in tumor development and progression. Posttranslational acetylation and deacetylation of histones, both epigenetic events regulated by histone acetyl transferases (HAT) and histone deacetylases (HDAC), respectively, control the expression and/or silencing of tumor suppressor genes.[1] While these two epigenetic regulators exist in equilibrium in non-transformed cells, HDAC activity predominates in most malignant tumors, effectively leading to silencing of tumor suppressor genes and uncontrolled proliferation of cancer cells.[2] Eighteen isoforms of HDAC are known, eleven of which depend on zinc for their catalytic activities and are group into: class I (HDACs 1–3 and 8); class II (subdivided into class II A (HDACs 4, 5, 7 and 9) and class IIB (HDACs 6 and 10)); and class IV (HDAC 11).[3] Class III HDACs, also known as sirtuins, are non-zinc dependent and require NAD^+ for their catalytic activity.[3b] The expression profiles of HDAC isoforms in different tumors vary with each isoform playing unique roles in driving tumorigenesis.[4] The therapeutic potential of HDAC inhibition has been validated by the US food and drugs administration's (FDA) approval of HDAC inhibitors (HDACi), vorinostat, romidepsin, belinostat and panabinostat (Fig. 1) for the treatment of cutaneous T-cell lymphoma, peripheral T-cell lymphoma and multiple myeloma.[5] Cardiotoxicity, short half-life, and inactivity towards solid tumors are few of many challenges faced by HDACi in the clinic.[3a,6]

Among the several drivers of inflammation in tumors, the inducible isoform of cyclooxygenases (COX), COX-2, plays a crucial role by ensuring a continuous supply of prostaglandin E2 (PGE_2) to the tumors.[7] The other COX isoform, COX-1, is constitutively expressed in the body where it performs housekeeping functions.[8] In contrast to COX-1, COX-2 expression is short-lived[9] and is upregulated in most tumors to meet up with the requirement for PGE_2 in the rapidly proliferating cells.[7b] Both COX isoforms facilitate the conversion of arachidonic acid to prostaglandin H2, which is in turn transformed to prostaglandins, by specific synthases, as required by the cells.[7b,10] Several COX inhibitors (Fig. 2), also

Abbreviations: HDAC, histone deacetylase; HDACi, histone deacetylase inhibitors; COX, cyclooxygenases; NSAIDs, non-steroidal anti-inflammatory drugs; AR, androgen receptor; ZBG, zinc binding group; PGE_2, prostaglandin E_2.

* Corresponding author at: School of Chemistry and Biochemistry, Georgia Institute of Technology, Atlanta, GA 30332-0400, USA.
E-mail address: aoyelere@gatech.edu (A.K. Oyelere).

http://dx.doi.org/10.1016/j.bmc.2016.12.032
0968-0896/

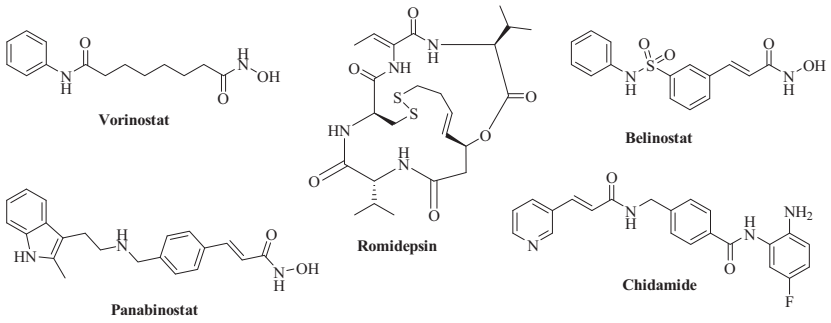

Fig. 1. HDACi in use in the clinic.

known as non-steroidal anti-inflammatory drugs (NSAIDs), have been approved by the FDA for managing inflammation associated with pains and fever.

Due to high expression of COX-2 in most tumors, it has been suggested that NSAIDs could someday find applications in the prevention and/or cure of some cancers, especially colon and prostate cancer.[11] Several mechanisms of cytotoxicity of NSAIDs towards cancer cells have been reported; most are believed to be independent of COX-2 inhibition. In androgen dependent prostate cancer cell line (LNCaP), celecoxib exerts its cytotoxic effect via induction of c-jun[12] and EP2 signaling leading to suppression of androgen receptor (AR).[13] Induction of apoptosis,[14] Wnt/beta-catenin pathway suppression,[15] cell cycle arrest[16] and inhibition of angiogenesis[17] are some of the other mechanisms through which NSAIDs exert their anticancer activity. In addition to being a possible therapeutic target, COX-2 upregulation in tumors has been exploited for tumor imaging through the use of contrast agents containing COX-2-selective NSAIDs.[18]

Recently, there has been enormous interest in the development of dual-acting compounds comprising of an HDACi and another cytotoxic component.[19] In such compounds, one of the "warheads" is usually the surface recognition group (cap) of the HDACi (see pharmacophoric model in Fig. 4a). While dual-acting compounds comprising NSAIDs and other agents exist,[20] none contain HDACi and NSAIDs combined as a single component. Moreover, results from *in vitro* studies suggest that enhanced cytotoxic effect could be achieved by combining NSAIDs and HDACi in cancer cell lines.[21] In this study, we designed and synthesized bifunctional compounds with HDAC and COX-2 inhibitory activities. These compounds are capable of harnessing the cytotoxic effects of HDAC inhibition, COX-2 inhibition, and perturbation of other non-COX dependent pathways. Our design has indomethacin or celecoxib as the cap, methylenes as linkers, and hydroxamate as the zinc binding group (ZBG) (Fig. 4b–e). These compounds potently inhibited the HDAC isoforms tested and retained COX-2 inhibitory activity comparable to both celecoxib and indomethacin. The potent HDAC and COX-2 inhibitory activities of these conjugates are reflected in their growth inhibitory activities in MCF-7 (breast cancer), A549 (non-small cell lung cancer), HCT-116 (colon cancer), DU-145 (androgen independent prostate cancer) and LNCaP (androgen dependent prostate cancer) cell lines. They are also less toxic towards healthy cell (VERO) compared to vorinostat.

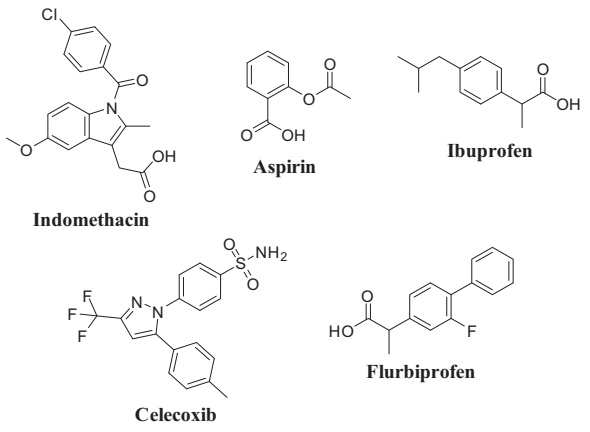

Fig. 2. Representative examples of US FDA approved NSAIDs.

2. Results and discussion

2.1. Design rationale

The residues presented at the outer rim of HDAC enzymes form rugged landscapes designed to flexibly accommodate a diverse class of substrates. This may explain the tolerance of the HDAC outer rim for incorporation of various surface recognition groups into the design of structurally dissimilar HDACi. Taking this into consideration, we hypothesized that incorporation of celecoxib (a COX-2 selective inhibitor) and indomethacin (a non-selective inhibitor of COX isoforms) into the surface recognition cap group of an HDACi may result in dual-acting agents that inhibit both HDAC and COX-2. Such agents are likely to show enhanced tumor cell cytotoxicity and superior therapeutic index compared to the individual HDACi and COX-2 inhibitors.

To determine which site to modify on celecoxib, we analyzed the orientation of celecoxib in the COX-2 active site. We found that the sulfonamide (SO_2NH_2) and trifluoromethyl (CF_3) moieties of celecoxib are projected towards different solvent exposed regions of the enzyme (Fig. 3a and b). Based on this analysis, the sulfonamide and trifluoromethyl moieties could be suitable points for the attachment of HDAC-inhibiting pharmacophores. Modifications at these two ends should minimally perturb the binding of celecoxib-based conjugates to the COX-2 active site, as shown in previous studies.[20b,22] Because of the relaxed specificity for hydrophobic groups at the HDAC outer rims, the celecoxib aromatic moiety of the resulting dual-acting agents is expected to be accommodated as a surface recognition group when bound to HDAC enzymes. To test this deduction, we designed and synthesized celecoxib-HDACi conjugates in which: (i) HDACi template is attached to the sulfonamide (series 1, Fig. 4), (ii), the "CF_3" is replaced by HDACi template (series 2, Fig. 4) and (iii) the sulfonamide is replaced with a methyl sulfone (SO_2Me) and "CF_3" is replaced by HDACi template (series 3, Fig. 4).

Similarly for indomethacin, the carboxylic acid moiety is projected towards the solvent exposed region of COX-2 (Fig. 3c). Modification of this moiety is known to convert indomethacin from a non-selective COX inhibitor to a COX-2 selective inhibitor.[23] This

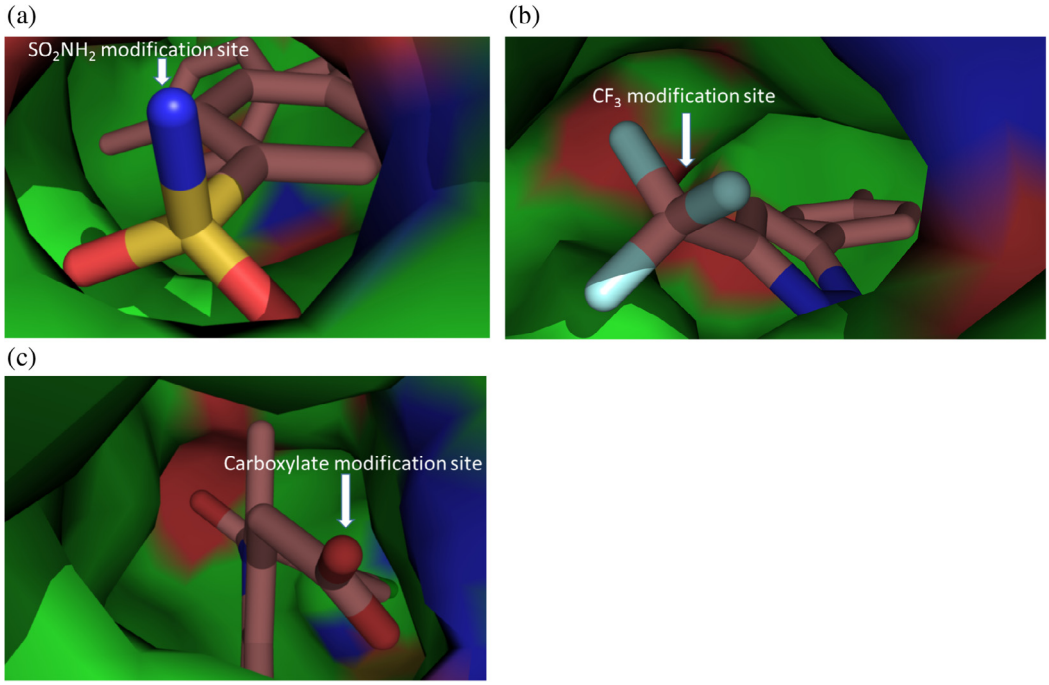

Fig. 3. Crystal structures showing (a) binding of celecoxib within COX-2 (PDB code 3LN1) showing SO_2NH_2 modification site, and (b) binding of celecoxib within COX-2 (PDB code 3LN1) showing CF_3 modification site, (c) binding of indomethacin within COX-2 (PDB code 4COX) showing carboxylate modification site.

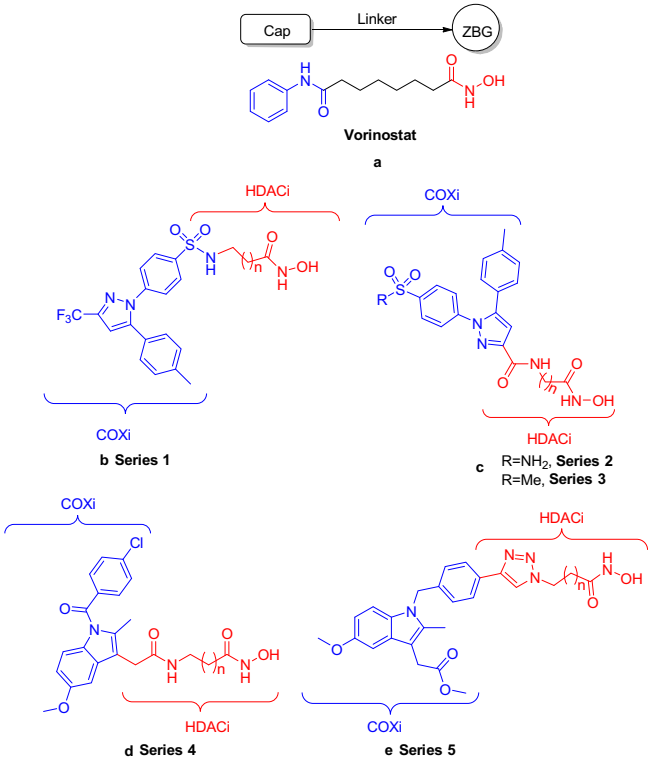

Fig. 4. (a) HDACi pharmacophoric model integrated in vorinostat structure. (b) Designed dual-acting COXi-HDACi compounds – (i) Celecoxib-based HDACi (series 1), (ii) and (iii) Celecoxib-based HDACi (series 2 and 3), (iv) and (v) Indomethacin-based HDACi (series 4 and 5).

prompted us to design and synthesize indomethacin-HDACi conjugates in which the HDACi template is attached to the carboxylic acid end (series 4, Fig. 4). Further modifications of indomethacin yielded conjugates in which the chlorobenzoyl is replaced by

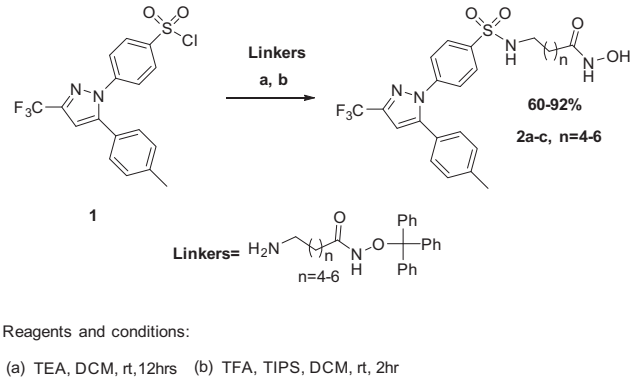

Scheme 1. Synthesis of series 1 celecoxib-HDACi conjugates.

HDACi template, and carboxylic acid is either esterified or left unmodified (series 5, Fig. 4).

In all the NSAID-HDACi conjugates, linker lengths were restricted to five, six and seven methylenes separating the ZBG from the cap groups, in accordance with a previous study in our lab showing these lengths to be optimal for HDAC inhibition.[24]

2.2. Chemistry

The sulfonyl chloride **1**, a vital intermediate required in the synthesis of sulfonamide-modified celecoxib-HDACi conjugates, was made according to a previously reported protocol.[25] The desired conjugates **2a–c** were thereafter made by displacement of chloride from compound **1** with trityl-protected primary amine having methylene linkers of appropriate lengths, followed by removal of trityl-protection with TFA (Scheme 1).

To access the series 2 conjugates, the 1-(4-sulfamoylphenyl)-5-(p-tolyl)-1H-pyrazole-3-carboxylic acid intermediate **5** was made by hydrolysis of ethyl 1-(4-sulfamoylphenyl)-5-(p-tolyl)-1H-pyra-

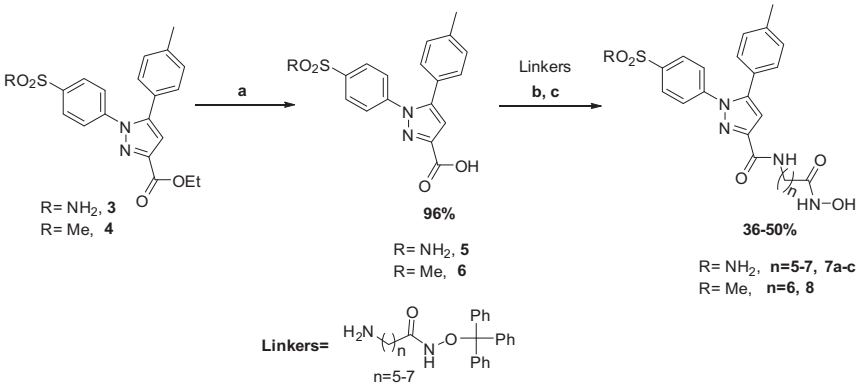

Scheme 2. Synthesis of series 2 and 3 celecoxib-HDACi conjugates.

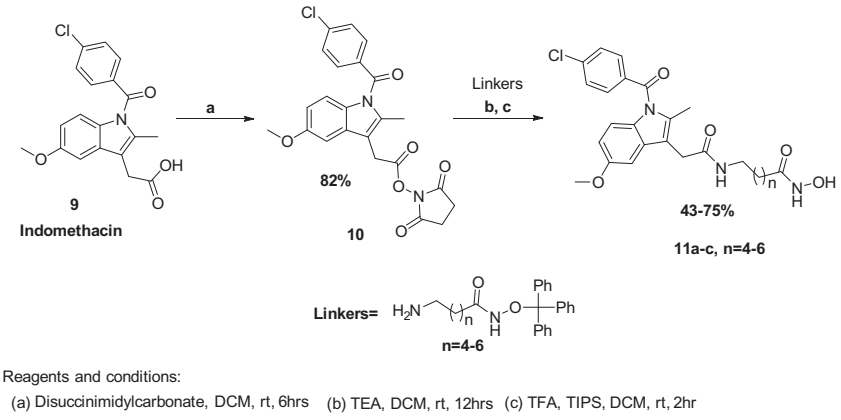

Scheme 3. Synthesis of series 4 celecoxib-HDACi conjugates.

zole-3-carboxylate **4**, whose synthesis had been previously reported,[26] using lithium hydroxide (Scheme 2). Subsequent coupling of compound **5** to trityl-protected primary amine having methylene linkers of appropriate lengths followed by trityl deprotection furnished the desired celecoxib-HDACi conjugates **7a–c** in decent yields. Likewise, the methyl sulfone analog **8** (series 3) was made from **6** using the same chemistry.

The first series of indomethacin-based COXi-HDACi conjugates (series 4) were made from the NHS-activated indomethacin intermediate **10**, which was obtained by reacting indomethacin with disuccinimidyl carbonate (Scheme 3). Displacement of NHS by trityl-protected primary amine having methylene linkers of appropriate lengths and subsequent trityl removal furnished conjugates **11a–c** in good yields.

The esterified indole **12** required to synthesize the second series of indomethacin-HDACi conjugates was obtained by hydrolysis of indomethacin using NaOH followed by esterification using TMSCl in MeOH. Reaction of **12** with 4-ethynylbenzyl mesylate **13** in the presence of sodium hydride, gave the *N*-alkylated alkyne intermediate **14** (Scheme 4). Via Cu (I) catalyzed azide-alkyne cycloaddition reaction between alkyne **14** and trityl-protected azide having methylene linkers of appropriate lengths **15a–c**, trityl-protected precursors to the final compounds **16** and **17a–c** were made. Ester hydrolysis with lithium hydroxide followed by trityl deprotection using TFA furnished the NSAID-HDACi conjugate **16** while methyl ester compounds **17a–c** were obtained by trityl deprotection of precursors to the final compounds (Scheme 4).

2.3. HDAC isoforms inhibition screening

We screened all of the synthesized dual-acting COXi-HDACi compounds against all class I HDACs (HDACs 1–3 and HDAC 8) and HDAC6 (class IIB HDAC). These conjugates potently inhibited all the HDAC isoforms screened. A closer look at the enzyme inhibitory activities reveals a linker length dependency which generally favors longer methylene linkers with few key exceptions (Table 1). Across all the five HDAC isoforms tested, these conjugates showed the strongest inhibitory effect towards HDAC 6, with IC_{50} as low as 5 nM for **17c**. Among the celecoxib-based series (series 1–2), compounds **7a–c** (series 2) showed more potency towards HDACs 1–3 compared to those of series 1 with the same linker lengths. This may be due to more favorable interaction of the 3′-amide and the free sulfonamide group, at the surface recognition group of conjugates, with potential H-bond donor/acceptor residues at the outer rim of the enzyme. In addition to the strong inhibitory effects towards HDAC 6 seen within the series 1 conjugates (compounds **2a–c**), **2b** also strongly inhibited HDACs 3 and 8, while **2c** showed preference for HDAC 3 compared to **2a** which has a strong inhibitory effect against HDAC 8. The only member of series 3 conjugates, compound **8**, is slightly more potent than compound **7b**, the corresponding conjugate in series 2 with the same linker length.

In the indomethacin-based series, conjugates with triazolyl connecting the linker to the head group, compounds **17a–c** (series 5), show greater inhibition of HDACs 1–3 and HDAC 6, compared to the amide-linked conjugates compounds **11a–c** (series 4). Com-

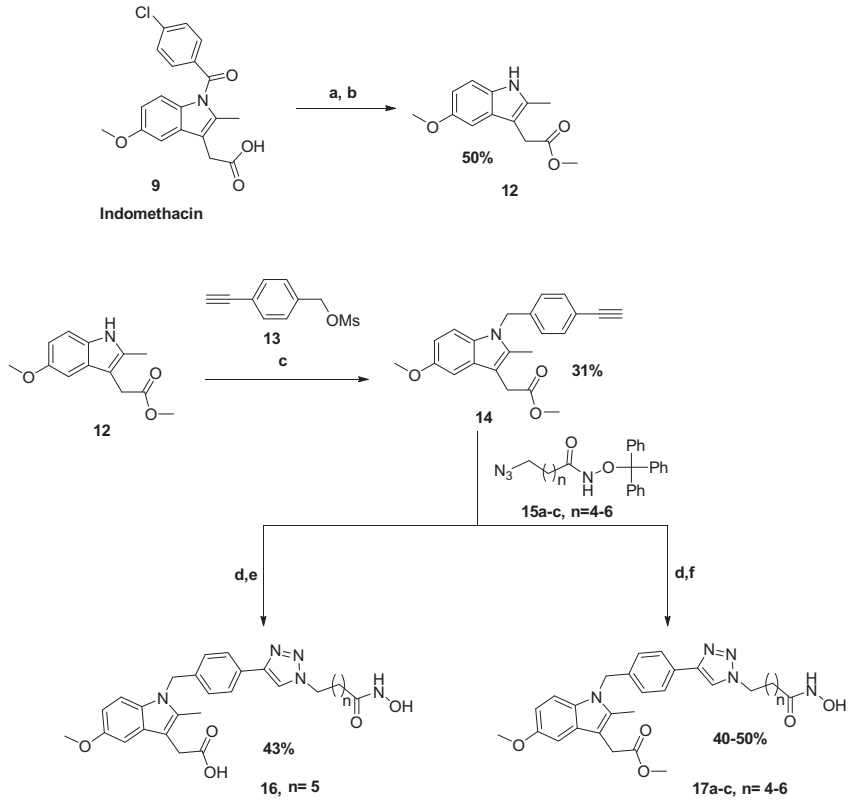

Reagents and conditions:
(a) NaOH, rt, 12 hrs (b) TMSCl, MeOH, rt, 12 hrs (c) NaH, THF, 0^0C-rt (d) CuI, DIPEA, THF, rt, 12 hrs (e) LiOH, THF/H_2O, rt, 12hrs (f) TFA, TIPS, DCM, rt, 2hr

Scheme 4. Synthesis of series 5 celecoxib-HDACi conjugates.

pounds **11a–c** are equipotent towards HDAC 6, while they show varying activities towards other HDAC isoforms. It is noteworthy to point out that compound **16** and its methyl ester analog **17b** show similar activity in all the HDAC isoforms screened, suggesting that modifying the carboxylic acid group in the series 5 conjugates does not result in loss of enzyme inhibitory activity. The remaining members of this series, **17a** and **17c**, have vastly varied anti-HDAC activities. Compound **17a** is moderately active against HDACs 3 and 8 with little activity against HDACs 1, 2 and 6. Conversely, **17c** is broadly active against all HDAC isoforms tested and it is the most potent HDAC 6 inhibitor among the dual-acting COXi-HDACi compounds herein disclosed.

2.4. Molecular docking analysis

To gain an insight into the specific interactions that may exist between our compounds and HDACs, which may explain the pattern of the observed HDAC inhibition, we docked all the compounds against HDAC 6. In all the series, we observed zinc chelation, typical of all hydroxamate-based HDACi, while the COX-binding moieties sit at surface of the enzyme (supporting information, Fig. S1).

In all the celecoxib-based conjugates (series 1–3), the "*para* tolyl" group makes a stabilizing pi-stacking interaction with PHE 680 residue at the surface of the enzyme. We observed that compound **2a**, analog with the shortest linker among the series 1 compounds, had the phenyl at the headgroup and the linker pushed further down the active site to maximize chelation with Zn at the bottom of the active site (supporting information, Fig. S1(i)). This slightly offset the pi-stacking interaction with PHE 680 at the surface of the enzyme, and may explain the slightly weaker activity against HDAC 6 compared to **2b** and **2c**. Compound **7b** had a slightly different orientation at the surface of the enzyme, with its "*para* tolyl" group and "phenyl sulfonamide groups flipped, but still maintained pi-stacking interaction with PHE 680 and Zn chelation shown by compounds **7a**, **7c** and **8** (supporting information, Fig. S1(iii)).

Among the indomethacin-based compounds, the series 4 conjugates, **11a–c**, adopt a similar binding pose within the HDAC 6 active site, except for **11c** (supporting information, Fig. S1(v)). Despite this, compounds **11a–c** have similar inhibitory effects on HDAC 6 (Table 1). All the series 5 conjugates, on the other hand, elicit a completely different interaction at the surface of the enzyme (supporting information, Fig. S1(vii)).

We also docked the conjugates against COX-2 to confirm that the structural modifications made on celecoxib and indomethacin do not appreciably compromise their interactions with COX-2. The selectivity of celecoxib towards COX-2 is attributed to its sulfonamide group forming four polar contacts (two H-bonding and two salt bridges) with His75, Arg499, Leu338 and Ser339 of COX-2, while the "*para* tolyl" group is projected towards the hydrophobic region in the active site.[27] Docking output of celecoxib-based series (series 1–3) show that the conjugates overlay perfectly with celecoxib in the COX-2 active site with the HDACi moiety projected towards the solvent exposed region. Among the series 1 conjugates, the "*para* tolyl" group is twisted perpendicularly to the plane of the "*para* tolyl" group of celecoxib (Fig. 5(i)), perhaps, to compensate for the modification at the sulfonamide end. The series 2

Table 1
HDAC isoforms inhibition screening (IC_{50} in nM)[a] of NSAIDs-HDACi conjugates.

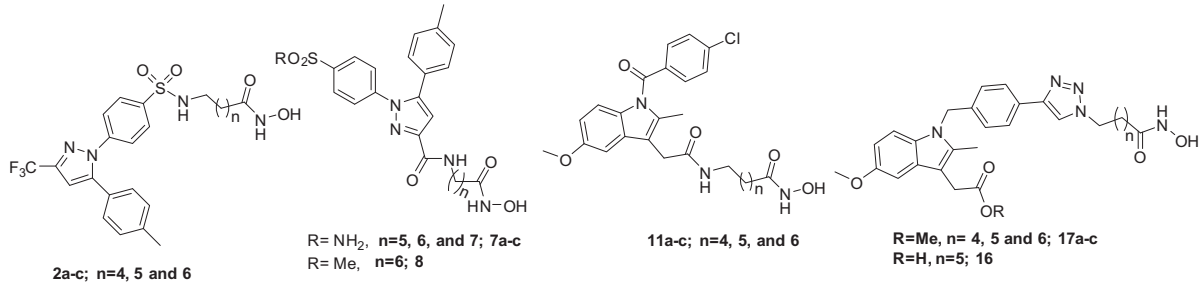

Compound	n	HDAC1	HDAC2	HDAC3	HDAC6	HDAC8
2a	4	1870 ± 280	2060 ± 400	1020 ± 160	76 ± 26	226 ± 90
2b	5	1030 ± 70	4050 ± 130	424 ± 53	66 ± 6	412 ± 43
2c	6	968 ± 160	929 ± 164	256 ± 35	61 ± 11	989 ± 142
7a	5	400 ± 60	232 ± 40	191 ± 44	92 ± 9	544 ± 76
7b	6	208 ± 52	294 ± 46	333 ± 79	83 ± 8	520 ± 110
7c	7	60 ± 7	32 ± 3	33 ± 8	183 ± 12	697 ± 55
8	6	261 ± 35	163 ± 8	338 ± 130	50 ± 16	345 ± 43
11a	4	1810 ± 330	41 ± 12%	722 ± 119	49 ± 10	345 ± 95
11b	5	980 ± 75	854 ± 280	356 ± 48	49 ± 9	109 ± 41
11c	6	1760 ± 190	43 ± 3%	283 ± 54	50 ± 14	707 ± 86
16	5	111 ± 15	302 ± 40	59 ± 10	22 ± 5	116 ± 32
17a	4	778 ± 105	1360 ± 530	224 ± 60	6830 ± 430	672 ± 77
17b	5	89 ± 13	407 ± 97	35 ± 6	10 ± 1	135 ± 35
17c	6	251 ± 80	209 ± 18	181 ± 71	5 ± 3	394 ± 172

% values refer to % inhibition at 10 μM.
[a] Average of three independent experiments.

conjugates on the other hand, align perfectly with celecoxib in the COX-2 active site, with the appended HDACi template projecting towards the solvent exposed region (Fig. 5(ii)). All the conjugates bind COX-2 similarly, irrespective of the length of the appended HDACi template.

A similar observation was seen with the indomethacin-based series 4 conjugates, wherein all the conjugates align with indomethacin, except for compound **11c**, with the HDACi appendage projected towards a pocket at the surface of the enzyme (Fig. 5 (iii) and (iv)). We believe the misalignment of compound **11c**, relative to indomethacin and other conjugates, is due to the length of the HDACi appendage. In order for the HDACi appendage to fit the pocket at the enzyme's surface, there has to be a distortion in the binding mode within the active site leading to the misalignment (Fig. 5(iii)). The Series 5 conjugates present a different binding mode, with the methyl ester group projected towards the hydrophobic region occupied by the chlorobenzoyl group of indomethacin. Consistent with previous observations in other series, all series 5 conjugates bind to the COX-2 active site in a similar fashion regardless of the length of the HDACi template.

2.5. COX inhibition study

We performed a preliminary screening (at 10 μM) of all the bifunctional compounds against COX-1 and COX-2 enzymes using Cayman fluorescent inhibitor screening assay kit. Based on the preliminary screen, representative members from each series were selected for IC_{50} determination in both COX isoforms (Table 2). In most cases, compounds within the same series showed similar percent inhibitory activities towards COX-1 and COX-2, validating our observation from docking which suggests that conjugates' within the same series should have similar interactions with COX-2, independent of the length of the HDACi appendage.

The celecoxib based conjugate **2b** retained selectivity towards COX-2 akin to celecoxib, though with reduced potency. Compound **7c** was surprisingly less potent compared to **2b** in the preliminary screen, despite having a near perfect alignment with celecoxib in the COX-2 active site (Fig. 5(ii)) compared to the alignment of **2b** (Fig. 5(i)). The only indomethacin-based compound evaluated for IC_{50}, **11b**, shows comparable level of potency towards COX-2 as indomethacin. Interestingly, the COX-2 selectivity of **11b** rivals that of celecoxib, an FDA-approved COX-2-selective inhibitor. The COX-2-selectivity seen with compound **11b** is consistent with observations in the literature on indomethacin modified at the carboxylic acid group.[23] Despite the drastic structural modifications to celecoxib and indomethacin templates which furnished compounds **8** and **17c** respectively, these compounds still showed decent activity towards COX-2 (Table 2).

2.6. In vitro anticancer activity study

Encouraged by the impressive HDAC and COX inhibitory activities of our conjugates, we tested their growth inhibitory activities in a panel of cancer cell lines: breast (MCF-7), lung (A549), colon (HCT-116), androgen-dependent (LNCaP) and -independent (DU-145) prostate cancer cell lines. Healthy monkey kidney epithelial cells (VERO) were used as a positive control. Our choice of cancer cell lines was based on the expression profiles of different HDAC isoforms and COX-2 in the cell lines. All class I HDACs and HDAC 6 (a class IIb HDAC) play crucial roles in the survival of the chosen cancer cell lines.[2,4] While COX-2 is ubiquitously expressed in the MCF-7[18a] and A549[30] cell lines, its expression is barely

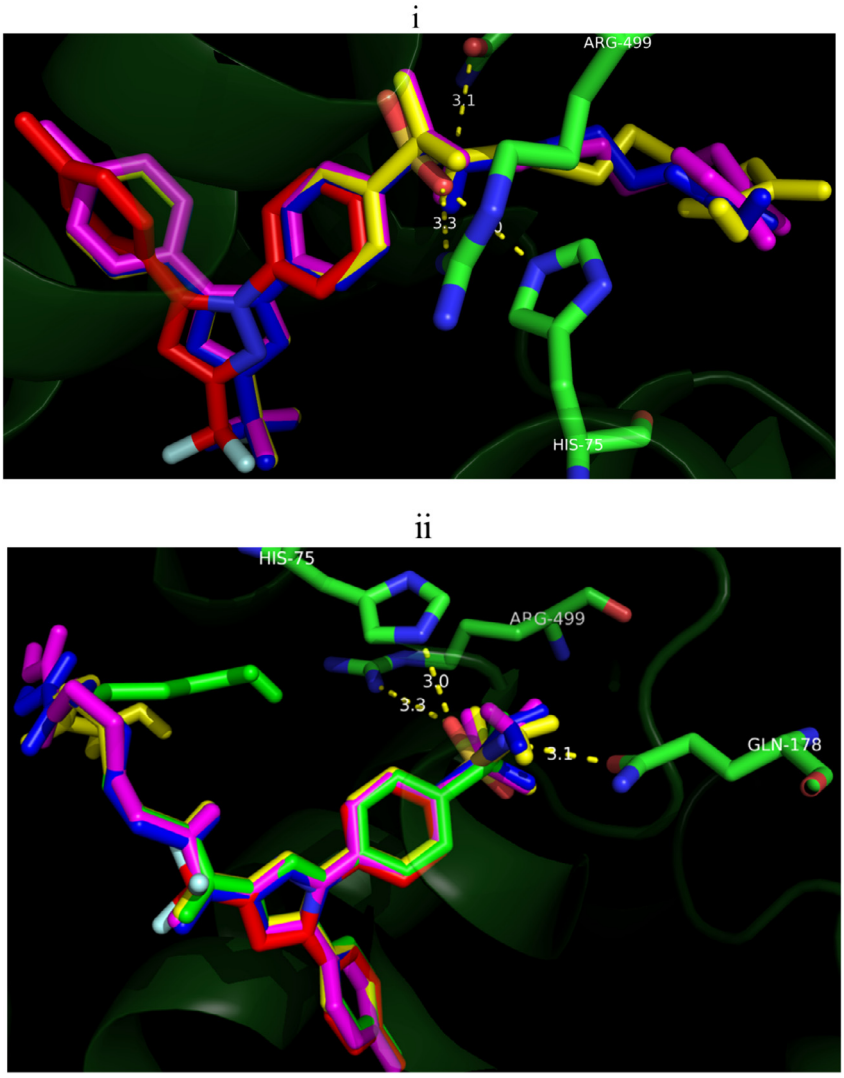

Fig. 5. Docking output of NSAID-HDACi conjugates overlaid with crystal structure of celecoxib and indomethacin in COX-2: (i) series 1 conjugates: **2a** (blue), **2b** (magenta), **2c** (yellow) and celecoxib (red); (ii) series 2 and 3 conjugates: **7a** (blue), **7b** (magenta), **7c** (yellow) **8** (green); (iii) series 4 conjugates: **11a** (blue), **11b** (magenta), **11c** (yellow), and indomethacin (red); (iv) surface representation of series 4 conjugates: **11a** (blue), **11b** (magenta), **11c** (yellow), and indomethacin (red); (v) series 5 conjugates: **17a** (blue), **17b** (magenta), **17c** (yellow), and indomethacin (red); (vi) surface representation of series 5 conjugates: **17a** (blue), **17b** (magenta), **17c** (yellow), and indomethacin (red).

discernible in the HCT-116,[22b] a colon cancer cell line that is highly sensitive to HDAC inhibition through COX-2 independent mechanism(s).[22c] Prostate cancer cell lines (LNCaP and DU-145) were chosen to evaluate the selectivity of our compounds towards androgen dependent prostate cancer. COX-2-specific NSAIDs perturb androgen receptor (AR)-mediated functions which are critical for the survival of LNCaP.[12] Most of the conjugates show strong antiproliferative effects in all the cancer cell lines used in this study, and are less cytotoxic towards VERO compared to SAHA. More specifically, we observed the compounds to be considerably more potent towards androgen dependent prostate (LNCaP) and HCT-116 (with no COX-2 expression).

Among the conjugates based on celecoxib (series 1–3), compounds **2a–c** show increasing activity with increase in methylene linker lengths in MCF-7 and A549 cell lines, consistent with the trend observed in their HDACs 1–3 and 6 inhibition activities. A different trend is observed for these series of compounds in HCT-116 and LNCaP cell lines, as compound **2b** potently inhibit the proliferation of both cell lines while **2c** is less potent against HCT-116 but equipotent as **2b** against LNCaP (Table 3). Surprisingly, sulfonamide compounds **7a–c** were barely cytotoxic across all cell lines (except for compound **7c**), despite their impressive anti-HDAC activities. The inactivity of the sulfonamide-based compounds **7a–c** may be due to lack of cell penetration to an appreciable extent. This deduction was supported by the fact that the methyl sulfone congener of inactive compound **7b**, compound **8**, showed anti-proliferative activity that is consistent with its HDAC inhibitory activity and with exquisite selectivity towards AR-positive LNCaP and HCT-116 cells.

Most of the indomethacin-based conjugates potently inhibited the growth of all the cancer cell lines, with the effect more pronounced within the series 5 conjugates (**17a–c**). Notably, compound **17c** showed IC_{50} comparable to vorinostat in A549 cell line and it is more cytotoxic towards LNCaP and HCT-116 in similar manner to the other active celecoxib-based compounds. Considering their strong anti-HDAC and weak COX-2 inhibitory effect within the series 5 conjugates, mechanism of cytotoxicity in HCT-116 could be attributed, predominantly, to HDAC inhibition. The series 4 conjugates **11b** and **11c** showed reduced anticancer effect in all cell lines, except LNCaP against which they are still potently active. Compound **11a**, the other member of this series,

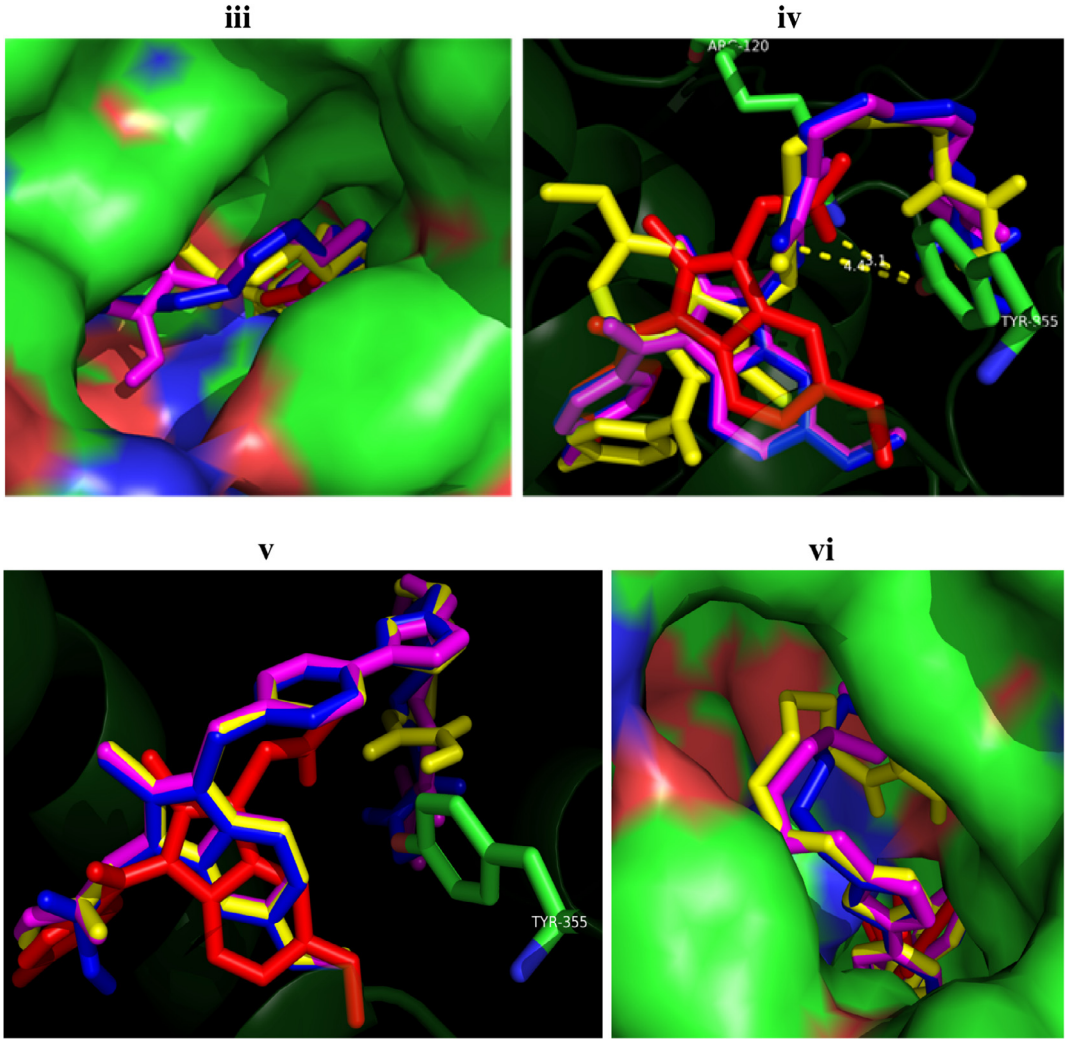

Fig. 5 (*continued*)

Table 2
COX isoforms inhibition study.

Compound	COX-1% inhibition[a]	COX-2% inhibition[a]	COX-1 IC_{50} (μM)[b]	COX-2 IC_{50} (μM)[b]	SI
2a	16.25	97.69	ND	ND	–
2b	61.43	100.00	3.57 ± 0.34	0.30 ± 0.03	>11
2c	26.05	95.57	ND	ND	–
7a	NI	19.06	ND	ND	–
7b	26.36	71.11	ND	ND	–
7c	NI	66.87	ND	ND	–
8	NI	60.25	23.09 ± 0.70	4.44 ± 0.06	>5.20
11a	40.22	95.13	ND	ND	–
11b	22.81	98.13	21.00 ± 9.07	0.33 ± 0.06	>60
11c	42.76	96.20	ND	ND	–
16	NI	40.59	ND	ND	–
17a	NI	11.51	ND	ND	–
17b	NI	50.77	ND	ND	–
17c	7.08	78.16	11.97 ± 1.10	4.58 ± 0.06	>2
Celecoxib	–	–	7.70[28]	0.07[28]	>100
Indomethacin	–	–	0.05[29]	0.20[29]	0.25

[a] Percent inhibition at 10 μM.
[b] Average of three independent experiments; NI represents no inhibition; ND represents not determined; SI represents selectivity index (COX-1 IC_{50}/COX-2 IC_{50}).

is poorly active or inactive against all cell lines tested. The cytotoxic effects of **11b** and **11c** towards LNCaP may be due to a combined effect of HDAC inhibition and inherent downregulation of AR associated with COX-2 selective NSAIDs.

In healthy cells (VERO), these compounds are significantly less toxic when compared to vorinostat. Specifically, compound **8** is about ten-fold more selective towards prostate cancer cells (LNCaP) compared to VERO. Likewise, compounds **11b**, **11c**, **17b**

Table 3
Cell growth inhibitory activity (IC_{50} in μM) of bifunctional COXi-HDACi conjugates in cancer and healthy cell line.[a]

Compound	MCF-7	A549	HCT-116	LNCaP	DU-145	Vero
2a	7.77 ± 1.20	10.44 ± 0.96	8.74 ± 0.23	8.88 ± 1.76	NT	6.83 ± 0.74
2b	5.70 ± 0.55	8.00 ± 0.23	3.38 ± 0.09	2.19 ± 0.21	6.41 ± 0.51	5.53 ± 0.40
2c	4.58 ± 0.23	8.15 ± 0.44	6.29 ± 0.15	2.11 ± 0.07	10.10 ± 0.33	6.61 ± 0.42
7a	>100	>100	NT	NT	NT	>100
7b	>100	>100	24.97 ± 1.95	>20	NT	>100
7c	59.48 ± 3.40	34.14 ± 7.43	7.12 ± 0.86	>20	NT	12.14 ± 0.34
8	16.34 ± 1.40	23.38 ± 2.60	2.62 ± 0.32	1.89 ± 0.11	18.30 ± 0.80	20.94 ± 1.26
11a	>100	31.93 ± 1.95	16.13 ± 0.79	>20	NT	40.67 ± 2.67
11b	29.30 ± 1.47	14.46 ± 1.76	11.21 ± 0.44	2.71 ± 0.52	7.26 ± 0.46	19.36 ± 1.36
11c	25.10 ± 9.38	33.02 ± 0.64	24.85 ± 1.11	6.46 ± 0.67	>20	34.74 ± 0.28
16	47.84%	NT	9.90 ± 1.95	NT	NT	NT
17a	14.16 ± 2.02	37.44 ± 1.03	9.31 ± 0.85	>20	NT	37.82 ± 1.26
17b	9.61 ± 1.45	8.22 ± 0.61	1.67 ± 0.09	1.35 ± 0.30	8.17 ± 0.05	5.82 ± 0.16
17c	5.94 ± 0.29	4.43 ± 0.14	1.28 ± 0.13	1.53 ± 0.51	12.54 ± 0.54	5.73 ± 0.29
SAHA	3.27 ± 0.05	5.00 ± 0.24	1.40	1.22 ± 0.06	3.45 ± 0.16	1.03 ± 0.09
Celecoxib	NT	NT	NT	32.60[12]	NT	NT
Indomethacin	5.20%	NT	NT	>300[12]	NT	NT

% represents percent inhibition at 100 μM, NT represents not tested.
[a] Average of three independent experiments.

and **17c** displayed varying level of selective cytotoxicity towards LNCaP compared to VERO.

2.7. Comparison of antiproliferative activity of bifunctional compounds and combination therapy of NSAIDs and HDACi

To investigate if there is an advantage in having bifunctional compounds compared to just a combination of the individual components (SAHA + Celecoxib; or SAHA + Indomethacin), we tested an equimolar concentration of the individual components, and compared their growth inhibitory activities to those of lead bifunctional compounds **2b** and **11b** in LNCaP, DU-145 and VERO. As shown in Fig. 6a above, compound **2b**, bifunctional compound derived from celecoxib template, is significantly more potent than a combination of celecoxib and SAHA in LNCaP, with no observable differences in DU-145 and VERO (Fig. 6b and c respectively). This confirms compound **2b** as a more selective and potent compound to treat AR positive prostate cancer. Indomethacin derived compound **11b** on the other hand, while equipotent to a combination of indomethacin and SAHA in both LNCaP and DU-147 (Fig. 6a and b respectively), is significantly less toxic to healthy cells, VERO (Fig. 6c). Hence, a hybrid of indomethacin and HDACi, **11b**, has a superior therapeutic index when compared to a combination of equimolar concentrations of indomethacin and SAHA.

Overall, compound **2b** is more potent (Fig. 6a) and selective towards LNCaP (Fig. S3a, supporting information) compared to compound **11b** and a combination of SAHA and the respective NSAID, while compound **11b** has the highest *in vitro* selective toxicity index.

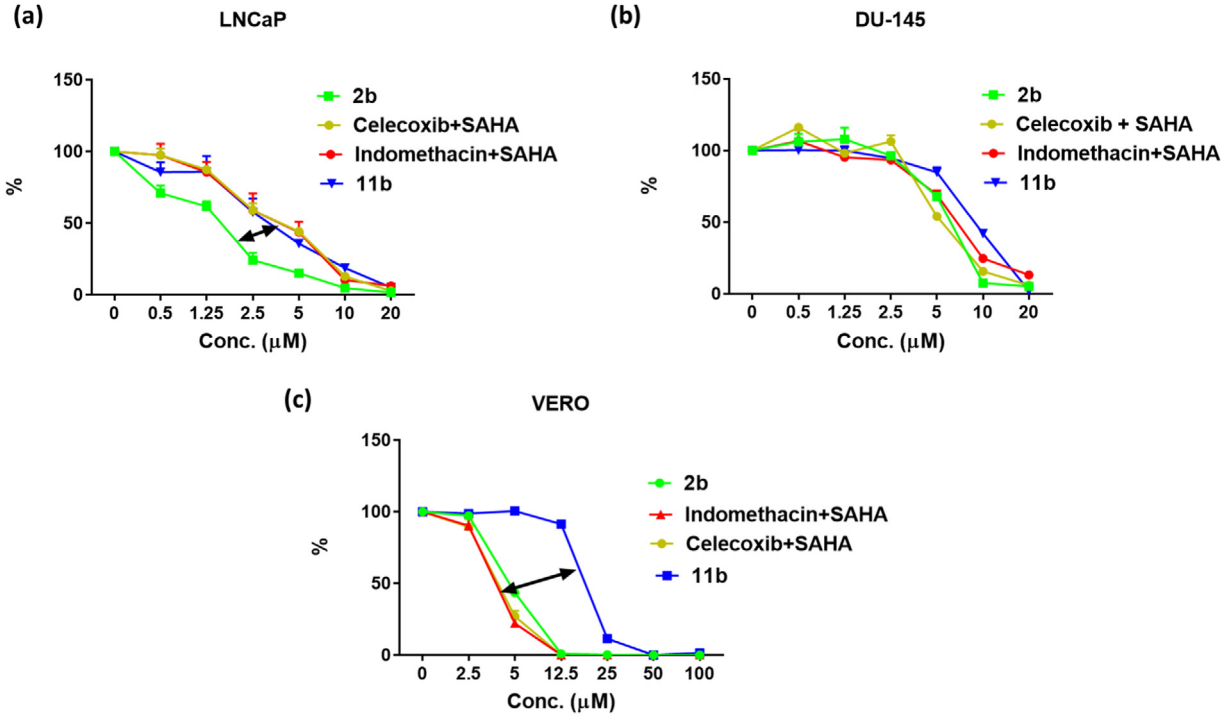

Fig. 6. Antiproliferative activity of combination of equimolar concentration of respective NSAIDs and SAHA compared to equal concentration of appropriate bifunctional compounds in (a) LNCaP; (b) DU-145; and (c) VERO cell lines.

2.8. Intracellular target validation

Using western blot, we probed for evidence of intracellular HDAC inhibition among our compounds in LNCaP. Inhibition of HDAC 6 is known to result in accumulation of acetylated tubulin in the cytosol.[31] In this experiment, we chose compound **2b** as a representative of all celecoxib-based conjugates (series 1–3), while compounds **11b** and **17b** were selected as representatives of series 4 and 5 conjugates respectively. SAHA was used as the positive control. As expected, all the tested compounds showed accumulation of acetylated tubulin in a concentration dependent manner (Fig. 7, panel 1). Compound **17b**, a highly potent HDAC 6 inhibitor ($IC_{50} \approx 10$ nM), showed about the same level of acetyl tubulin at 1.5 μM (Fig. 7, panel 1, lane **7**) as SAHA at 10 μM (Fig. 7, panel 1, lane 2). A similar trend was observed with histone H4 acetylation (a marker of class 1 HDAC inhibition) (see supporting information Fig. S2).

According to Yamaguchi et al.[32], HDAC inhibition causes downregulation of PMA-induced COX-2 expression in cancer cell lines. A similar observation was obtained when we treated LNCaP cells with SAHA at 10 μM (Fig. 7, panel 3, lane 2). Our observation, following treatment with compounds **11b** and **17b**, was contrary to this, as we saw sustained COX-2 expression levels at the tested concentrations (Fig. 7, panel 3, lanes 5–7). Compound **2b**, on the other hand, showed COX-2 downregulation at low concentration (2 μM) and a slight upregulation a higher concentration (10 μM) (Fig. 7, panel 3, lanes 3–4). The implication of this may be that the cytotoxic effect of these compounds in LNCaP may be less dependent on their effects on COX-2 expression. This is not without precedence, as other selective COX-2 inhibitors are known to induce apoptosis independent of COX-2 expression.[14,33] However, the sustained COX-2 expression level observed with our compounds, clearly distinguishes them from SAHA. This may prove to be advantageous in *in vivo* experiments with prostate cancer, as the COX-2 binding component of our compounds may confer selective localization in the tumor.

AR upregulation is critical to the survival of LNCaP.[34] In our study with LNCaP, SAHA significantly suppressed AR expression at 10 μM (Fig. 7, panel 2, lane 2), consistent with the literature.[35] Compounds **2b** showed a similar effect in a concentration dependent manner (Fig. 7, panel 2, lanes 3–4). Quite unexpectedly, AR downregulation was much weaker for compound **11b** (Fig. 7, panel 2, lanes 5–6), while compound **17b** showed no noticeable effect at the single concentration tested (Fig. 7, panel 2, lane **7**). Both celecoxib and indomethacin showed no effects on AR regulation at 10 μM (Fig. 7, panel 2, lanes 8 and 9). All together, these observations suggest that our compounds might be perturbing distinct pathways to elicit anti-proliferative activities against LNCaP cells. Compound **2b** acts more like a typical HDACi via induction protein acetylation and downregulation of AR. In contrast, **11b** and **17b** are atypical as they have no effect on AR expression. They most likely derived their potent anti-proliferative effect on LNCaP cells through a combination of COX-2-facilitated cell uptake, HDAC inhibition and perturbation of other pathways unique to prostate cancer.

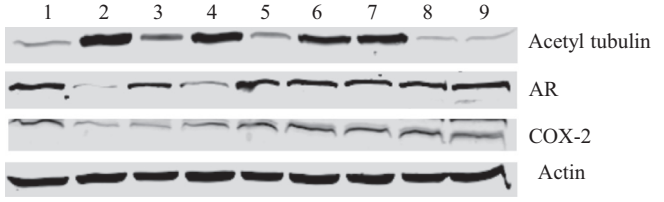

Fig. 7. Western blot analysis of acetylated tubulin, AR and COX-2 in LNCaP following treatment for 24 h. Lanes: 1, Control (DMSO); 2, SAHA (10 μM); 3, **2b** (2 μM); 4, **2b** (10 μM); 5, **11b** (2 μM); 6, **11b** (10 μM); 7, **17b** (1.5 μM); 8, celecoxib (10 μM); 9, indomethacin (10 μM).

2.9. Effect of bifunctional compounds on PGE_2 expression

One of the consequences on intracellular COX inhibition is decreased production of prostaglandin E2 (PGE_2).[36] To confirm that the strong COX-2 inhibitory effects of our compounds is maintained in cells, we treated HeLa cells with compounds **2b**, **11b**, celecoxib and indomethacin for 24 h then measured the level of PGE_2 produced in the cell culture supernatant. HeLa cell line was chosen for this study because it has been previously used for a similar study[36] (see Table S1 supporting information for the IC_{50} of these compounds in HeLa cells). As shown in Fig. 8, both compounds **2b** and **11b** significantly inhibited PGE_2 production, confirming that these NSAID-HDACi conjugates possess intracellular COX-2 inhibitory activities as well.

2.10. Effect of lead compound on cell cycle progression

To determine if the potent cell proliferation inhibition activities of these compounds result from their perturbation of the cell cycle pattern, we evaluated the effect of compounds **2a**, **8**, **11b** and **17b** on LNCaP cell cycle progression using SAHA, celecoxib and indomethacin as controls. We observed that the effect of celecoxib and indomethacin (both at 40 μM) was not significantly different from the DMSO control. SAHA at 2.5 μM induced a G_0/G_1 phase arrest as reported previously in the literature[35] (Fig. 9). Compound **8**, at 2.5 μM, displayed a similar G_0/G_1 phase arrest as SAHA. This is not unexpected, since **8** has a broad HDAC inhibition activity and only weak inhibitory effect against COX-2 (Table 2). Compared to **8**, compounds **2a**, **11b** and **17b**, have a distinct effect on cell cycle progression. At 2.5 μM, they induced a significant S phase arrest. This may be as a result of their combined HDAC and COX-2 inhibitory effects.

2.11. Bifunctional compounds suppress NTHi-induced NF-κB activation

NF-κB activation drives inflammation and tumorigenesis in cancer. The two pathways involved in NF-κB activation (canonical and non-canonical pathways) are initiated by pro-inflammatory cytokines such as TNFα and interleukins.[37] We recently reported

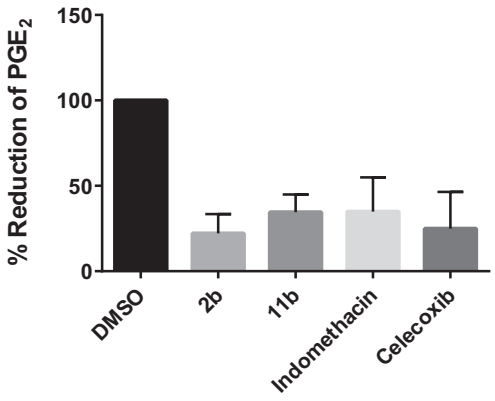

Fig. 8. Intracellular COX-2 inhibition is evidenced by attenuation of prostaglandin E2 (PGE_2) production. HeLa cells were treated with each of the tested compounds at 10× IC_{50} (Table 2) for 24 h and PGE_2 level was measured. Celecoxib and indomethacin were tested at 0.1 μM and 0.2 μM respectively. Data are representative of three independent experiments.

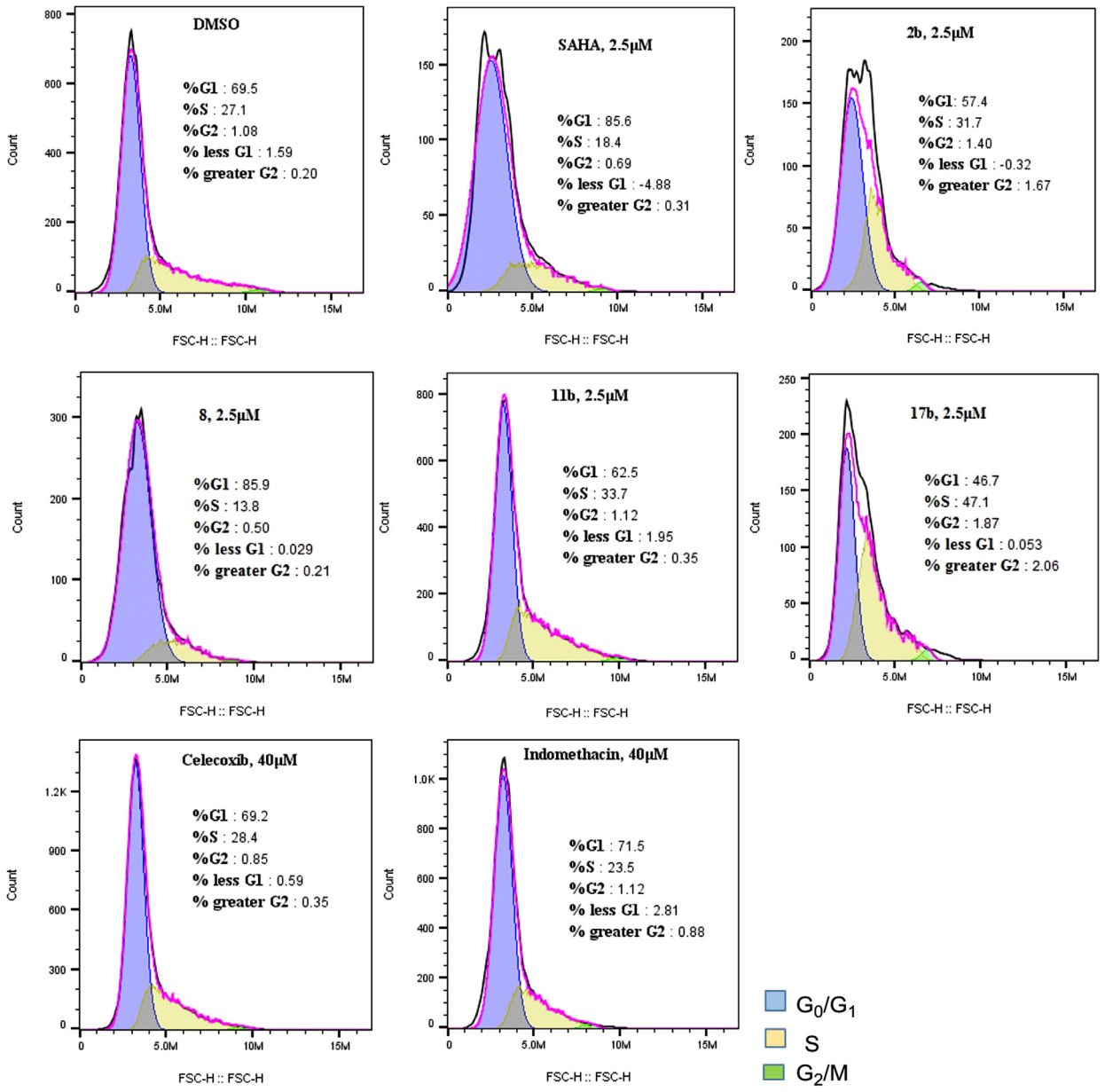

Fig. 9. Effect of SAHA, **2b**, **8**, **11b**, **17b**, celecoxib and indomethacin on LNCaP cell cycle progression.

that HDACi downregulate inflammatory cytokines release and NF-κB activation.[38] Likewise, there is evidence for non-COX inhibition dependent downregulation of NF-κB activation by NSAIDs.[39] In view of these, we investigated the ability of our bifunctional compounds to suppress NF-κB activation in BEAS-2B cells treated with nontypeable *Haemophilus influenzae* (NTHi) using NF-κB luciferase assay. NTHi is a Gram-negative bacterium which causes infection in the human respiratory tract. NF-κB is potently activated upon NTHi infection in human epithelial cells, and induces pro-inflammatory mediators such as IL-1β, IL-6 and TNF-α.

We screened representative NSAID-HDACi conjugates with potent HDAC inhibition activities and observed that compounds **8** and **17b** suppressed NTHi-induced NF-κB activation in BEAS-2B cells almost to the same extent as SAHA (Fig. 10). In this assay, compound **2c**, celecoxib and indomethacin also showed some level of suppression of NF-κB (Fig. S5, supporting information). Considering the fact that compounds **8** and **17b** have moderate COX and strong HDAC inhibitory activities, their ability to downregulate NF-κB activation is likely a consequence of their HDAC inhibitory

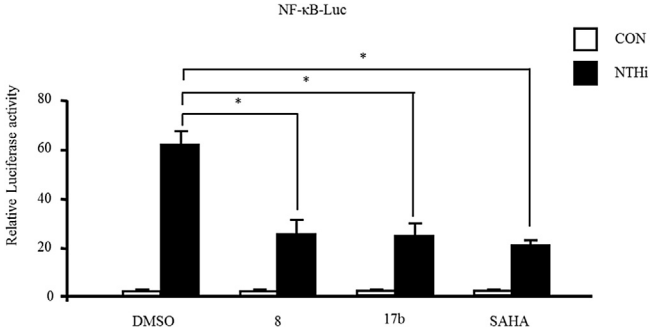

Fig. 10. Representative NSAID-HDACi conjugates inhibit NF-κB activation. BEAS-2B cells, transfected with NF-κB luciferase construct, were pre-treated with compounds **8**, **17b** or SAHA at 1 μM for 1 h and stimulated with NTHi for 5 h, and NF-kB promoter activity was then measured by performing luciferase assay. Data are mean ± SD (n = 3). $^{*}p < 0.05$. Statistical analysis was performed using Student's *t*-test. Data are representative of three independent experiments. CON = BEAS-2B cells treated with PBS control; NTHi = BEAS-2B cells treated with NTHi.

capability. In summary, these results demonstrate that representative NSAID-HDACi conjugates could suppress inflammation due to their ability to inhibit NF-κB activation.

3. Conclusion

The clinical success of HDACi as a single agent in the treatment of solid tumors continues to remain elusive. Approaches currently exploited to make this achievable include: (i) using a non-hydroxamate ZBG,[40] (ii) having a targeting group attached to the surface recognition group,[19a] (iii) making dual acting conjugates comprising a cytotoxic component and HDACi template,[19a] and (iv) using a prodrug approach.[41] Herein, we described compounds that potently and selectively inhibit COX-2 while also maintaining strong anti-HDAC activity. In addition to exploiting the anticancer effects of the two enzyme inhibitory templates in our design, we anticipate that these compounds may show selective localization in tumors as seen with other conjugates comprising a COX-2-selective inhibitor and a fluorophore.[18a,18c,22b,42] This approach has led to the discovery of compounds with strong growth inhibitory activities in various cancer cell lines with a strong preference for androgen-dependent prostate cancer cell line (LNCaP). While the selectivity towards LNCaP is not fully understood, we postulate that it could be a consequence of the effect of COX-2 and HDAC inhibition on AR functions. Previous studies on the effect of NSAIDs on AR in LNCaP suggest that COX-2 inhibition led to induction of the transcription factor c-jun, which in turn results in inhibition of AR activity.[12] HDAC inhibition on the other hand, leads to decreased AR expression.[35]

Compared to SAHA, our lead compounds (**2b**, **2c**, **8**, **11b**, **17b** and **17c**) showed superior *in vitro* therapeutic index in all cancer cell lines relative to the positive control VERO. Compounds **8** and **11b** are particularly impressive in this regard, with about a ten-fold increase in selective cytotoxicity towards LNCaP relative to VERO. Lastly, we observed significant differences in the perturbation of cell cycle progression by compounds **2b**, **11b** and **17b**, compared to SAHA, celecoxib and indomethacin that may be due to their combined effects on COX-2 and HDAC.

4. Experimental

4.1. Materials and methods

All commercially available starting materials were used without further purification. Indomethacin was purchased from TCI America (OR, USA). Reaction solvents were either high performance liquid chromatography (HPLC) grade or American Chemical Society (ACS) grade and used without further purification. Analtech silica gel plates (60 F_{254}) were used for analytical TLC, and Analtech preparative TLC plates (UV 254, 2000 μm) were used for purification. UV light was used to examine the spots. 200–400 mesh silica gel was used in column chromatography. For NMR spectra, Varian-Gemini 400 MHz or Bruker 500 MHz magnetic resonance spectrometer was used. ^{1}H NMR spectra were recorded in parts per million (ppm) relative to the peak of $CDCl_3$, (7.26 ppm), CD_3OD (3.31 ppm), or DMSO-d_6 (2.49 ppm). ^{13}C spectra were recorded relative to the central peak of the $CDCl_3$ triplet (77.0 ppm), CD_3OD (49.0 ppm), or the DMSO-d_6 septet (39.7 ppm) and were recorded with complete heterodecoupling. Multiplicities are described using the abbreviations: s, singlet; d, doublet, t, triplet; q, quartet; m, multiplet. High-resolution mass spectra were recorded at the Georgia Institute of Technology mass spectrometry facility in Atlanta. HPLC was used to establish the purity of the compounds to be >95%. The HPLC analyses were done on a Beckman Coulter instrument with a Phenomenex RP C-18 column (250 mm × 4.6 mm), using 0.1% TFA in water (solvent A) and 0.1% TFA in acetonitrile (solvent B), starting with 70% B for 5 min, then a gradient decrease of 70–10% of B over 20 min. The flow rate was 1.0 mL/min and detection was at 280 nm. 4-Ethynyl-benzyl methylsulfonate **13**, trityl-protected azide and amine linkers were made as previously described.[43]

Du-145, LNCaP, Vero and A549 cell lines were purchased from ATCC (Manassas, VA), while MCF-7 and HCT-116 were generous a gifts from Dr. Al Merrill's and Dr. Julia Kubanek's laboratories respectively, at Georgia Institute of technology, Atlanta, GA. Cell cultures were maintained in an incubator at 37 °C under a 5% CO_2 atmosphere. Mouse antiacetylated α-tubulin antibody was obtained from Invitrogen (Life Technologies, Grand Island, NY, USA), rabbit antiactin, and rabbit antitubulin α antibodies were purchased from Sigma-Aldrich (St. Louis, MO, USA), AR antibody was purchased from Cell Signaling, while COX-2 antibody was purchased from Cayman chemicals. Secondary antibodies, goat antirabbit conjugated to IRDye680, and goat antimouse conjugated to IRDye800 were purchased from LI-COR Biosciences (Lincoln, NE, USA). The CellTiter 96 Aqueous One Solution Cell Proliferation assay (MTS) kit was purchased from Promega (Madison, WI, USA).

4.1.1. N-Hydroxy-6-((4-(5-(p-tolyl)-3-(trifluoromethyl)-1H-pyrazol-1-yl) phenyl) sulfonamido) hexanamide (**2a**)

Triethylamine (0.02 mL, 0.175 mmol) was added to a solution of trityl-protected 6-aminohexanehydroxamic acid (0.05 g, 0.13 mmol) in $CHCl_3$ (10 mL) and left to stir under argon for 5 min. Thereafter, a solution of 4-(5-(p-tolyl)-3-(trifluoromethyl)-1H-pyrazol-1-yl) benzenesulfonyl chloride (0.05 g, 0.13 mmol) in anhydrous $CHCl_3$ (5 mL) was added and the reaction left to stir overnight. Reaction was quenched with water (20 mL) and extracted with DCM (20 mL) three times. Combined organic layers were dried over anhydrous sodium sulfate and concentrated in vacuo. Residue was purified with prep TLC to give 6-((4-(5-(p-tolyl)-3-(trifluoromethyl)-1H-pyrazol-1-yl) phenyl)sulfonamido)-N-(trityloxy)hexanamide an off-white solid (0.08 g, 0.10 mmol) which was immediately used for the next reaction without characterization.

To a solution of 6-((4-(5-(p-tolyl)-3-(trifluoromethyl)-1H-pyrazol-1-yl) phenyl)sulfonamido)-N-(trityloxy)hexanamide (0.08 g, 0.10 mmol) in anhydrous DCM (10 mL) were added TFA (1.5 mL) and TIPS (0.75 mL). Reaction was stirred at room temperature for 1 h. Solvent was evaporated and the resulting residue purified by prep TLC using DCM:Acetone:AcOH (2:1:0.1) to give **2a** as an off-white solid (0.03 g, 60%). HPLC retention time 16.22 min. ^{1}H NMR (400 MHz, CD_3OD) δ 7.90 (d, J = 8.5 Hz, 2H), 7.54 (d, J = 8.5 Hz, 2H), 7.21 (q, J = 8.2 Hz, 4H), 6.94 (s, 1H), 2.90 (t, J = 6.8 Hz, 2H), 2.38 (s, 3H), 2.09 (m, 2H), 1.60 (m, 2H), 1.54–1.45 (m, 2H), 1.34 (m, 2H). ^{13}C NMR (101 MHz, CD_3OD) δ 145.7, 143.5, 142.6, 142.1, 140.7, 139.8, 129.2, 128.6, 127.6, 125.7, 124.4, 122.3, 105.6, 42.5, 28.9, 25.8, 25.6, 24.8, 19.9. HRMS (ESI) $[M+H]^+$ calculated for $[C_{23}H_{26}O_4N_4F_3S]^+$ was 511.1621, found 511.1608.

4.1.2. N-Hydroxy-7-((4-(5-(p-tolyl)-3-(trifluoromethyl)-1H-pyrazol-1-yl)phenyl)sulfonamido) heptanamide (**2b**)

Trityl-protected 7-aminoheptanehydroxamic acid (0.05 g, 0.14 mmol) was reacted with 4-(5-(p-tolyl)-3-(trifluoromethyl)-1H-pyrazol-1-yl) benzenesulfonyl chloride (0.05 g, 0.13 mmol) in anhydrous $CHCl_3$ (5 mL) containing TEA (0.03 mL, 1.87 mmol) similar to compound **2a** above, to give 7-((4-(5-(p-tolyl)-3-(trifluoromethyl)-1H-pyrazol-1-yl)phenyl)sulfonamido)-N-(trityloxy) hexanamide as an off-white solid (0.08 g, 0.11 mmol) which was used for the next reaction (trityl deprotection) without characterization.

Trityl deprotection was done as described for **2a** in a DCM (10 mL) solution containing TFA (1.5 mL) and TIPS (0.75 mL).

Purification was by prep TLC using DCM:Acetone:AcOH (2:1:0.1) to give **2b** as an off-white solid (0.05 g, 92%). HPLC retention time 16.22 min. ^{1}H NMR (500 MHz, CD_3OD) δ 7.89 (d, J = 8.1 Hz, 2H), 7.53 (d, J = 8.1 Hz, 2H), 7.21 (dd, J = 18.5, 7.7 Hz, 4H), 6.93 (s, 1H), 2.89 (t, J = 6.5 Hz, 2H), 2.37 (s, 3H), 2.10 (s, 2H), 1.60 (s, 2H), 1.47 (s, 2H), 1.32 (s, 5H). ^{13}C NMR (126 MHz, MeOD) δ 145.7, 143.7, 143.3, 142.2, 140.8, 139.7, 129.1, 128.7, 127.7, 125.8, 122.4, 120.2, 105.5, 42.6, 29.1, 28.2, 27.8, 25.9, 25.2, 19.9. HRMS (ESI) $[M+H]^+$ calculated for $[C_{24}H_{28}O_4N_4F_3S]^+$ was 525.1778, found 525.1771.

4.1.3. N-Hydroxy-7-((4-(5-(p-tolyl)-3-(trifluoromethyl)-1H-pyrazol-1-yl)phenyl)sulfonamido) octanamide (**2c**)

Trityl-protected 8-aminooctanehydroxamic acid (0.06 g, 0.14 mmol) was reacted with 4-(5-(p-tolyl)-3-(trifluoromethyl)-1H-pyrazol-1-yl) benzenesulfonyl chloride (0.05 g, 0.13 mmol) in anhydrous $CHCl_3$ (5 mL) containing TEA (0.03 mL, 1.87 mmol) similar to compound **2a** above, to give 8-((4-(5-(p-tolyl)-3-(trifluoromethyl)-1H-pyrazol-1-yl)phenyl)sulfonamido)-N-(trityloxy) octanamide an off-white solid (0.09 g, 0.11 mmol) which was used for the next reaction (trityl deprotection) without characterization.

Trityl deprotection was done as described for **2a** in a DCM (10 mL) solution containing TFA (1.5 mL) and TIPS (0.75 mL). Purification was by prep TLC using DCM:Acetone:AcOH (2:1:0.1) to give **2c** as an off-white solid (0.04 g, 71%). HPLC retention time 16.82 min. ^{1}H NMR (400 MHz, CD_3OD) δ 7.86 (d, J = 7.3 Hz, 2H), 7.50 (d, J = 7.6 Hz, 2H), 7.17 (dd, J = 14.9, 8.0 Hz, 4H), 6.91 (s, 1H), 2.85 (s, 2H), 2.34 (s, 3H), 1.58 (m, 2H), 1.43 (m, 2H), 1.26 (m, J = 14.1 Hz, 8H). ^{13}C NMR (101 MHz, cd$_3$od) δ 145.7, 143.4, 143.1, 142.1, 140.7, 139.6, 129.2, 128.6, 127.6, 125.7, 122.5, 119.9, 105.5, 42.6, 29.1, 28.5, 28.4, 26.2, 25.7, 19.9. HRMS (ESI) $[M+H]^+$ calculated for $[C_{25}H_{30}O_4N_4F_3S]^+$ was 539.1934, found 539.1928.

4.1.4. 1-(4-Sulfamoylphenyl)-5-(p-tolyl)-1H-pyrazole-3-carboxylic acid (**5**)

Ethyl 1-(4-sulfamoylphenyl)-5-(p-tolyl)-1H-pyrazole-3-carboxylate (1.33 g, 3.31 mmol) was dissolved in THF (30 mL) and $LiOH{\cdot}H_2O$ (0.21 g, 4.97 mmol) was added followed by 6 mL of H_2O. The reaction was left to stir at room temperature overnight.·THF was evaporated off and product was precipitated off the resulting solution with 1 N HCl. Precipitate was filtered and washed severally with H_2O to give (**5**) as a white solid (1.14 g, 96%). ^{1}H NMR (400 MHz, DMSO-d_6) δ 13.15 (s, 1H), 7.91 (d, J = 8.6 Hz, 2H), 7.56 (d, J = 8.8 Hz, 4H), 7.23 (q, J = 8.2 Hz, 4H), 7.09 (s, 1H), 2.34 (s, 3H). ^{13}C NMR (101 MHz, DMSO-d_6) δ 163.9, 146.2, 145.6, 144.5, 142.6, 139.7, 130.4, 129.7, 127.8, 127.0, 126.8, 111.1, 21.8.

4.1.5. 1-(4-(Methylsulfonyl)phenyl)-5-(p-tolyl)-1H-pyrazole-3-carboxylic acid (**6**)

Ethyl 1-(4-(methylsulfonyl)phenyl)-5-(p-tolyl)-1H-pyrazole-3-carboxylate (0.42 g, 1.08 mmol) was reacted with $LiOH{\cdot}H_2O$ (0.09 g, 2.16 mmol) following the same procedure for **5** above to give **6** as a white solid (0.38 g, 100%). ^{1}H NMR (400 MHz, DMSO-d_6) δ 8.03 (d, J = 8.7 Hz, 2H), 7.61 (d, J = 8.6 Hz, 2H), 7.26–7.17 (m, 4H), 7.09 (s, 1H), 3.31 (s, 3H), 2.33 (s, 3H). ^{13}C NMR (101 MHz, DMSO-d_6) δ 163.4, 145.8, 145.1, 143.5, 140.6, 139.3, 129.9, 129.2, 128.7, 126.5, 126.3, 110.8, 43.7, 21.2.

4.1.6. N-(6-(Hydroxyamino)-6-oxohexyl)-1-(4-sulfamoylphenyl)-5-(p-tolyl)-1H-pyrazole-3-carboxamide (**7a**)

EDCI (0.03 g, 0.17 mmol) and HOBT (0.02 g, 0.17 mmol) were added to a solution of 1-(4-sulfamoylphenyl)-5-(p-tolyl)-1H-pyrazole-3-carboxylic acid (**5**) (0.05 g, 0.14 mmol) in $CHCl_3$ (10 mL). The mixture was stirred at room temperature for 30 min after which trityl-protected 6-aminohexanehydroxamic acid (0.06 g, 0.154 mmol) was added, then left to stir overnight. The reaction was quenched with $NaHCO_3$ (20 mL) and extracted three times with DCM (20 mL). Combined organic layer was dried over anhydrous Na_2SO_4 and concentrated *in vacuo*. Crude product was purified by prep TLC using DCM:Acetone:AcOH (5:1:0.1) to give N-(6-oxo-6-(trityloxy)amino)hexyl)-1-(4-sulfamoylphenyl)-5-(p-tolyl)-1H-pyrazole-3-carboxamide, which was used for the next reaction (trityl deprotection) without characterization.

To a solution of N-(6-oxo-6-(trityloxy)amino)hexyl)-1-(4-sulfamoylphenyl)-5-(p-tolyl)-1H-pyrazole-3-carboxamide (0.06 g, 0.08 mmol) in anhydrous DCM (10 mL), TFA (1.5 mL) and TIPS (0.75 mL) were added. Reaction was stirred at room temperature for 1 h. Solvent was evaporated and the resulting residue purified by prep TLC using DCM:MeOH:AcOH (10:1:0.1) to give **7a** as an off white solid (0.03 g, 50%). HPLC retention time 9.47 min. ^{1}H NMR (500 MHz, DMSO-d_6) δ 8.58 (s, 1H), 8.09 (d, J = 8.1 Hz, 2H), 7.75 (d, J = 8.4 Hz, 2H), 7.42 (dd, J = 18.1, 7.9 Hz, 4H), 7.20 (s, 1H), 5.98 (s, 1H), 3.47 (d, J = 5.5 Hz, 2H), 2.54 (s, 3H), 1.73 (m, J = 6.7 Hz, 3H), 1.47 (m, J = 14.0 Hz, 3H). ^{13}C NMR (126 MHz, DMSO-d_6) δ 161.6, 148.7, 145.3, 144.3, 142.6, 139.3, 130.2, 129.5, 127.4, 126.6, 108.8, 55.8, 30.1, 29.8, 27.5, 26.8, 25.7, 25.1, 21.7. HRMS (ESI) $[M+H]^+$ calculated for $[C_{23}H_{28}O_5N_5S]^+$ was 486.1806, found 486.1804.

4.1.7. N-(7-(Hydroxyamino)-7-oxoheptyl)-1-(4-sulfamoylphenyl)-5-(p-tolyl)-1H-pyrazole-3-carboxamide (**7b**)

Trityl-protected 7-aminoheptanehydroxamic acid (0.08 g, 0.16 mmol) was reacted with a solution of 1-(4-sulfamoylphenyl)-5-(p-tolyl)-1H-pyrazole-3-carboxylic acid (**5**) (0.05 g, 0.14 mmol), HOBT (0.02 g, 0.17 mmol) and EDCI (0.03 g, 0.17 mmol) in $CHCl_3$ (10 mL) similar to compound **7a** above, to give N-(7-oxo-7-((trityloxy)amino)heptyl)-1-(4-sulfamoylphenyl)-5-(p-tolyl)-1H-pyrazole-3-carboxamide as an brown solid (0.08 g, 0.11 mmol) which was used for the next reaction (trityl deprotection) without characterization.

Trityl deprotection was done as described for **7a**. Purification was by prep TLC using DCM:MeOH:AcOH (10:1:0.1) to give **7b** as a brown solid (0.02 g, 36%). HPLC retention time 10.13 min. ^{1}H NMR (500 MHz, DMSO-d_6) δ 8.34 (s, 1H), 7.87 (d, J = 8.4 Hz, 2H), 7.53 (d, J = 8.4 Hz, 2H), 7.20 (dd, J = 18.1, 8.1 Hz, 4H), 6.98 (s, 1H), 3.25 (d, J = 3.3 Hz, 2H), 2.32 (s, 3H), 1.95 (m, 2H), 1.50 (m, 4H), 1.26 (m, J = 19.3 Hz, 4H). ^{13}C NMR (126 MHz, DMSO) δ 161.9, 149.1, 145.7, 144.5, 142.8, 139.7, 130.5, 129.7, 127.7, 127.3, 126.9, 109.2, 39.6, 30.3, 29.5, 27.3, 26.3, 26.2, 21.9. HRMS (ESI) $[M+H]^+$ calculated for $[C_{24}H_{30}O_5N_5S]^+$ was 500.1962, found 500.1956.

4.1.8. N-(8-(Hydroxyamino)-8-oxooctyl)-1-(4-sulfamoylphenyl)-5-(p-tolyl)-1H-pyrazole-3-carboxamide (**7c**)

Trityl-protected 8-aminooctanehydroxamic acid (0.06 g, 0.15 mmol) was reacted with a solution of 1-(4-sulfamoylphenyl)-5-(p-tolyl)-1H-pyrazole-3-carboxylic acid (**5**) (0.05 g, 0.14 mmol), HOBT (0.02 g, 0.17 mmol) and EDCI (0.03 g, 0.17 mmol) in $CHCl_3$ (10 mL), as described for compound **7a** above, to give N-(8-oxo-8-((trityloxy)amino)octyl)-1-(4-sulfamoylphenyl)-5-(p-tolyl)-1H-pyrazole-3-carboxamide as an brown solid (0.08 g, 0.11 mmol) which was used for the next reaction (trityl deprotection) without characterization.

Trityl deprotection was done as described for **7a**. Purification was by prep TLC using DCM:MeOH:AcOH (10:1:0.1) to give **7c** as a brown solid (0.02 g, 36%). HPLC retention time 10.92 min. ^{1}H NMR (500 MHz, DMSO-d_6) δ 8.37 (s, 1H), 7.90 (d, J = 8.1 Hz, 2H), 7.56 (d, J = 8.1 Hz, 2H), 7.23 (dd, J = 18.1, 7.9 Hz, 4H), 7.01 (s, 1H), 3.28 (s, 2H), 2.35 (s, 3H), 1.97 (m, 2H), 1.54 (m, 4H), 1.29 (m, J = 21.0 Hz, 8H). ^{13}C NMR (126 MHz, DMSO) δ 161.3, 148.5, 144.9, 143.8, 142.1, 139.1, 129.9, 129.1, 127.2, 126.7, 126.2, 108.4, 35.3,

31.9, 29.6, 29.0, 28.2, 26.8, 21.3. HRMS (ESI) $[M+H]^+$ calculated for $[C_{25}H_{32}O_5N_5S]^+$ was 514.2119, found 514.2106.

4.1.9. N-(7-(Hydroxyamino)-7-oxoheptyl)-1-(4-(methylsulfonyl) phenyl)-5-(p-tolyl)-1H-pyrazole-3-carboxamide (**8**)

Trityl-protected 7-aminoheptanehydroxamic acid (0.12 g, 0.31 mmol) was reacted with a solution of 1-(4-(methylsulfonyl) phenyl)-5-(p-tolyl)-1H-pyrazole-3-carboxylic acid (**6**) (0.10 g, 0.28 mmol), HOBT (0.04 g, 0.31 mmol) and EDCI (0.06 g, 0.30 mmol) in $CHCl_3$ (10 mL) as described for compound **7a** above, to give 1-(4-(methylsulfonyl)phenyl)-N-(7-oxo-7-((trityloxy) amino)heptyl)-5-(p-tolyl)-1H-pyrazole-3-carboxamide as an brown solid (0.08 g, 0.11 mmol) which was used for the next reaction (trityl deprotection) without characterization.

Trityl deprotection was done as described for **7a**. Purification was by prep TLC using DCM:MeOH:AcOH (10:1:0.1) to give **8** as a brown solid (0.02 g, 36%). HPLC retention time 11.13 min. ^{1}H NMR (400 MHz, dmso) δ 8.41 (s, 1H), 8.03 (d, J = 8.4 Hz, 2H), 7.63 (d, J = 8.4 Hz, 2H), 7.24 (q, J = 8.3 Hz, 4H), 7.01 (s, 1H), 3.31 (s, 3H), 2.35 (s, 3H), 2.04 (m, 2H), 1.93 (m, 2H), 1.54 (m, 4H), 1.31 (m, 4H). ^{13}C NMR (101 MHz, DMSO-d_6) δ 156.2, 148.5, 144.9, 143.5, 140.4, 139.2, 129.9, 129.1, 128.5, 126.6, 126.3, 109.0, 105.0, 43.8, 32.3, 29.6, 28.7, 26.6, 25.6, 21.3. HRMS (ESI) $[M+H]^+$ calculated for $[C_{25}H_{31}O_5N_4S]^+$ was 499.2010, found 499.2010.

4.1.10. NHS-activated indomethacin (**10**)

Disuccinimidyl carbonate (0.86 g, 3.35 mmol) was added to a mixture of indomethacin (1.00 g, 2.79 mmol) and TEA (0.50 mL, 3.35 mmol) in DCM (20 mL). The reaction was stirred at room temperature overnight. Solvent was evaporated off and the residue purified by column chromatography using DCM: Acetone (10:1) to give **10** as a white solid (1.04 g, 82%). ^{1}H NMR (400 MHz, $CDCl_3$) δ 7.68–7.63 (m, 2H), 7.49–7.43 (m, 2H), 6.97 (d, J = 2.5 Hz, 1H), 6.94–6.89 (m, 1H), 6.69 (dd, J = 9.0, 2.5 Hz, 1H), 3.96 (s, 2H), 3.85 (s, 3H), 2.80 (s, 4H), 2.37 (s, 3H). ^{13}C NMR (101 MHz, $CDCl_3$) δ 169.1, 168.6, 166.5, 156.4, 139.6, 136.6, 133.9, 131.6, 130.9, 130.2, 129.3, 115.3, 112.8, 110.4, 100.9, 55.9, 27.4, 25.8, 13.7.

4.1.11. 6-(2-(1-(4-Chlorobenzoyl)-5-hydroxy-2-methyl-1H-indol-3-yl)acetamido)-N-hydroxyhexanamide (**11a**)

TEA (0.02 mL, 0.16 mmol) was added to a solution of NHS-activated indomethacin **10** (0.05 g, 0.11 mmol) and trityl-protected 7-aminoheptanehydroxamic acid (0.05 g, 0.12 mmol) in DCM (10 mL). The reaction was left to stir at room temperature for 3 h. The reaction was quenched with water (20 mL) and extracted three times with DCM (20 mL). Combined organic layer was dried over Na_2SO_4 and concentrated *in vacuo*. Residue obtained was purified by prep TLC using DCM: Acetone (10:1) to give 6-(2-(1-(4-chlorobenzoyl)-5-methoxy-2-methyl-1H-indol-3-yl)acetamido)-N-(trityloxy)hexanamide (0.07 g, 81%) which was used for the next reaction (trityl deprotection) without characterization.

Trityl group deprotection was done by dissolving 6-(2-(1-(4-chlorobenzoyl)-5-methoxy-2-methyl-1H-indol-3-yl)acetamido)-N-(trityloxy)hexanamide in anhydrous DCM (10 mL) after which 1.5 mL TFA and 0.5 mL TIPS were added and the reaction was left to stir for 2 h. Saturated $NaHCO_3$ solution (40 mL) was added to the reaction and extracted three times with DCM (20 mL) after gas evolution had ceased. Combined organic layer was dried over Na_2SO_4 and concentrated *in vacuo*. Crude residue was purified by prep TLC using DCM:Acetone:AcOH (2:1:0.1) to give **11a** as a light brown solid (0.07 g, 75%). HPLC retention time 12.82 min. ^{1}H NMR (400 MHz, CD_3OD) δ 7.72 (d, J = 8.4 Hz, 2H), 7.58 (d, J = 8.4 Hz, 2H), 7.03 (d, J = 2.2 Hz, 1H), 6.95 (d, J = 9.0 Hz, 1H), 6.70 (dd, J = 9.0, 2.3 Hz, 1H), 3.86–3.80 (m, 3H), 3.62 (s, 2H), 3.22 (t, J = 6.7 Hz, 2H), 2.34 (s, 3H), 2.08 (s, 2H), 1.58 (d, J = 33.3 Hz, 4H), 1.32 (d, J = 9.7 Hz, 2H). ^{13}C NMR (101 MHz, CD_3OD) δ 168.6, 164.9, 156.2, 138.7, 135.7, 134.3, 131.0, 130.7, 128.8, 114.5, 113.5, 111.1, 104.4, 101.0, 54.8, 52.8, 39.1, 30.9, 28.6, 26.0, 24.9, 12.3. HRMS (ESI) $[M+H]^+$ calculated for $[C_{25}H_{29}O_5N_3Cl]^+$ was 486.1790, found 486.1782.

4.1.12. 7-(2-(1-(4-Chlorobenzoyl)-5-methoxy-2-methyl-1H-indol-3-yl)acetamido)-N-hydroxyheptanamide (**11b**)

Reaction of NHS-activated indomethacin **10** (0.10 g, 0.22 mmol) with trityl-protected 7-aminoheptanehydroxamic acid (0.10 g, 0.24 mmol) in DCM (10 mL) containing TEA (0.04 mL, 0.26 mmol), as described for **11a**, gave 7-(2-(1-(4-chlorobenzoyl)-5-methoxy-2-methyl-1H-indol-3-yl)acetamido)-N-(trityloxy)heptanamide (0.14 g, 87%). Trityl deprotection was achieved as described for **11a** to give **11b** as a light brown solid (0.14 g, 87%). HPLC retention time 13.25 min. ^{1}H NMR (400 MHz, DMSO-d_6) δ 10.40 (s, 1H), 8.77 (s, 1H), 8.09 (s, 1H), 7.70 (dd, J = 17.6, 8.5 Hz, 4H), 7.15 (d, J = 2.3 Hz, 1H), 6.97 (d, J = 9.0 Hz, 1H), 6.74 (dd, J = 9.0, 2.4 Hz, 1H), 3.83–3.76 (m, 3H), 3.52 (s, 2H), 3.40 (s, 1H), 3.07 (d, J = 5.9 Hz, 2H), 2.32–2.21 (m, 3H), 1.95 (t, J = 7.3 Hz, 2H), 1.46 (dd, J = 18.5, 11.6 Hz, 4H), 1.25 (m, 4H). ^{13}C NMR (101 MHz, DMSO-d_6) δ 169.7, 169.1, 168.3, 156.0, 138.0, 135.6, 134.8, 131.6, 131.2, 131.0, 130.7, 129.6, 114.9, 111.6, 102.4, 55.8, 49.9, 32.7, 31.6, 29.4, 28.9, 26.6, 25.7, 14.0. HRMS (ESI) $[M+H]^+$ calculated for $[C_{26}H_{31}O_5N_3Cl]^+$ was 500.1947, found 500.1935.

4.1.13. 8-(2-(1-(4-Chlorobenzoyl)-5-methoxy-2-methyl-1H-indol-3-yl)acetamido)-N-hydroxyoctanamide (**11c**)

Reaction of NHS-activated indomethacin **10** (0.05 g, 0.11 mmol) with trityl-protected 7-aminoheptanehydroxamic acid (0.05 g, 0.12 mmol) in DCM (10 mL) containing TEA (0.02 mL, 0.16 mmol), as described for **11a**, gave 8-(2-(1-(4-chlorobenzoyl)-5-methoxy-2-methyl-1H-indol-3-yl)acetamido)-N-(trityloxy)octanamide (0.08 g, 91%). Trityl deprotection was achieved as described for **11a** to give **11c** as a light brown solid (0.02 g, 47%). HPLC retention time 13.95 min. ^{1}H NMR (400 MHz, CD_3OD) δ 7.69 (d, J = 8.1 Hz, 2H), 7.55 (d, J = 8.1 Hz, 2H), 7.00 (s, 1H), 6.92 (d, J = 8.9 Hz, 1H), 6.67 (d, J = 8.7 Hz, 1H), 5.49 (s, 2H), 3.80 (s, 3H), 3.59 (s, 2H), 3.19 (d, J = 5.5 Hz, 2H), 2.31 (s, 3H), 1.52 (m, J = 28.6 Hz, 4H), 1.26 (m, J = 14.7 Hz, 8H). ^{13}C NMR (101 MHz, CD_3OD) δ 170.9, 169.2, 162.8, 158.5, 149.8, 147.4, 141.0, 138.0, 136.6, 133.2, 131.1, 116.8, 115.7, 113.6, 103.3, 57.1, 55.7, 44.5, 43.8, 41.4, 33.4, 31.0, 30.8, 28.8, 14.5. HRMS (ESI) $[M+H]^+$ calculated for $[C_{27}H_{33}O_5N_3Cl]^+$ was 514.2103, found 514.2087.

4.1.14. Methyl 2-(5-methoxy-2-methyl-1H-indol-3-yl)acetate (**12**)

Indomethacin (3.00 g, 8.39 mmol) was dissolved in 1 M NaOH (200 mL) and left to stir overnight. The reaction was acidified with 1 M HCl and the precipitate filtered off. Filtrate was then extracted three times with DCM (100 mL). Combined organic layer was dried over Na_2SO_4 and concentrated *in vacuo* to give crude 2-(5-methoxy-2-methyl-1H-indol-3-yl)acetic acid (1.12 g, 5.15 mmol). The crude intermediate was dissolved in MeOH (50 mL) and TMSCl (1.86 mL, 14.73 mmol) was added. The reaction mixture was left to stir at room temperature overnight. Water (50 mL) was added to quench the reaction and extracted three times with DCM (50 mL). Organic layer was combined, dried over Na_2SO_4 and concentrated *in vacuo*. Residue obtained was purified by column chromatography using $CHCl_3$:EtOAc (10:1) to give **12** as a brown solid (0.99 g, 83%). ^{1}H NMR (400 MHz, $CDCl_3$) δ 7.92 (s, 1H), 7.07 (d, J = 8.7 Hz, 1H), 7.01 (d, J = 2.0 Hz, 1H), 6.81–6.75 (m, 1H), 3.87 (d, J = 1.1 Hz, 3H), 3.68 (d, J = 1.0 Hz, 5H), 2.32 (s, 3H). ^{13}C NMR (101 MHz, $CDCl_3$) δ 172.8, 154.1, 133.7, 130.2, 129.0, 111.1, 110.8, 104.1, 100.4, 55.9, 51.9, 30.3, 11.7.

*4.1.15. Methyl 2-(1-(4-ethynylbenzyl)-5-methoxy-2-methyl-1H-indol-3-yl)acetate (**14**)*

A solution of methyl 2-(5-methoxy-2-methyl-1H-indol-3-yl)acetate (**12**) (0.10 g, 0.43 mmol) and NaH (60% dispersion in mineral oil) (0.03 g, 0.64 mmol) in anhydrous THF (10 mL) was cooled to 0 °C and left to stir for 20 min. The reaction was brought to room temperature, after which 4-ethynylbenzyl methanesulfonate (0.11 g, 0.51 mmol) was added, and left to stir overnight. Reaction mixture was poured into sat. NH_4Cl (10 mL) and extracted three times with DCM (15 mL). Combined organic layer was dried over Na_2SO_4 and concentrated *in vacuo*. Purification was by prep TLC using $CHCl_3$:Ether (20:1) to give **14** as a yellow solid (0.05 g, 31%). ^{1}H NMR (400 MHz, $CDCl_3$) δ 7.41 (d, J = 8.0 Hz, 2H), 7.15–7.10 (m, 2H), 6.85 (d, J = 8.0 Hz, 2H), 6.80–6.78 (m, 1H), 5.36 (s, 2H), 3.87 (s, 3H), 3.73 (s, 2H), 3.69 (s, 3H), 3.08 (s, 1H), 2.31 (s, 3H). ^{13}C NMR (101 MHz, $CDCl_3$) δ 172.8, 154.1, 138.1, 135.0, 133.7, 130.2, 129.0, 128.0, 125.0, 121.6, 111.1, 110.8, 104.1, 100.4, 83.4, 55.9, 51.9, 46.8, 30.3, 11.7. HRMS (ESI) $[M+H]^+$ calculated for $[C_{22}H_{21}NO_3]^+$ was 347.1521, found 347.1529.

*4.1.16. 2-(1-(4-(1-(7-(Hydroxyamino)-7-oxoheptyl)-1H-1,2,3-triazol-4-yl)benzyl)-5-methoxy-2-methyl-1H-indol-3-yl)acetic acid (**16**)*

Methyl 2-(1-(4-ethynylbenzyl)-5-methoxy-2-methyl-1H-indol-3-yl)acetate (**14**) (0.074 g, 0.21 mmol), trityl-protected 7-azidoheptanehydroxamic acid (0.11 g, 0.26 mmol) and DIPEA (0.07 mL, 0.43 mmol) were dissolved in anhydrous THF (10 mL) and purged for 10 min at room temperature while stirring. CuI (0.02 g, 0.11 mmol) was then added with purging continued for another 20 min. The reaction was left to stir overnight. Reaction was quenched with a solution of 4:1 sat. NH_4Cl/NH_4OH (20 mL) and extracted with a mixture of 10% MeOH in DCM (3×) (20 mL). Combined organic layer was dried over anhydrous Na_2SO_4 and concentrated *in vacuo*. Purification was by prep TLC using 10:1 DCM:MeOH to give methyl 2-(5-methoxy-2-methyl-1-(4-(1-(7-oxo-7-((trityloxy)amino)heptyl)-1H-1,2,3-triazol-4-yl)benzyl)-1H-indol-3-yl)acetate (0.08 g, 51%), which was used for the next reaction.

The product of the first step above was dissolved in a 4:1 MeOH/H_2O mixture (5 mL). $LiOH{\cdot}H_2O$ (0.0065 g, 0.16 mmol) was added to the solution which was left to stir for 6 h. Solvent was evaporated off and the residue purified by prep TLC using EtOAc:hexane:AcOH (2:1:0.1) to give 2-(5-methoxy-2-methyl-1-(4-(1-(7-oxo-7-((trityloxy)amino)heptyl)-1H-1,2,3-triazol-4-yl)benzyl)-1H-indol-3-yl)acetic acid (0.035 g, 45%) as a yellow solid. Trityl deprotection was done as described for **11a**. Purification was done using 10:1:0.1 DCM:MeOH:AcOH to give **16** as a yellow solid (0.023 g, 96%). HPLC retention time 10.62 min. ^{1}H NMR (500 MHz, DMSO-d_6) δ 10.38 (s, 1H), 8.53 (s, 1H), 7.76 (s, 2H), 7.29 (s, 1H), 7.06 (d, J = 18.4 Hz, 3H), 6.70 (d, J = 7.5 Hz, 1H), 5.40 (s, 2H), 4.40 (s, 2H), 3.80 (d, J = 22.4 Hz, 3H), 3.55 (s, 2H), 2.32 (s, 3H), 1.92 (d, J = 30.5 Hz, 2H), 1.49 (s, 2H), 1.28 (s, 5H). ^{13}C NMR (126 MHz, DMSO-d_6) δ 184.2, 175.2, 171.2, 163.3, 156.1, 148.5, 144.5, 139.8, 136.8, 135.4, 131.5, 129.9, 124.8, 120.1, 115.3, 110.8, 91.9, 65.6, 59.5, 56.1, 39.6, 35.9, 35.0, 22.4, 15.0. HRMS (ESI) $[M+H]^+$ calculated for $[C_{28}H_{34}O_5N_5]^+$ was 520.2554, found 520.2549.

*4.1.17. Methyl 2-(1-(4-(1-(6-(hydroxyamino)-6-oxohexyl)-1H-1,2,3-triazol-4-yl)benzyl)-5-methoxy-2-methyl-1H-indol-3-yl)acetate (**17a**)*

Reaction of methyl 2-(1-(4-ethynylbenzyl)-5-methoxy-2-methyl-1H-indol-3-yl)acetate (**14**) (0.070 g, 0.20 mmol) with trityl-protected 6-azidohexanehydroxamic acid (0.10 g, 0.24 mmol) in the presence of DIPEA (0.070 mL, 0.43 mmol) and CuI (0.019 g, 0.10 mmol) in THF (10 mL), as described above for **16**, gave methyl 2-(5-methoxy-2-methyl-1-(4-(1-(6-oxo-6-((trityloxy)amino)hexyl)-1H-1,2,3-triazol-4-yl)benzyl)-1H-indol-3-yl)acetate (0.075 g, 49%). Trityl deprotection was achieved as described for **11a**. Purification was done by prep TLC using 10:1 DCM:MeOH to give **17a** as a brown solid (0.042 g, 40%). HPLC retention time 12.88 min. ^{1}H NMR (400 MHz, CD_3OD) δ 8.13 (s, 1H), 7.62 (d, J = 8.1 Hz, 2H), 7.08 (d, J = 8.8 Hz, 1H), 6.96 (dd, J = 11.0, 5.2 Hz, 3H), 6.67 (dd, J = 8.8, 2.3 Hz, 1H), 5.26 (s, 2H), 4.33 (t, J = 6.9 Hz, 2H), 3.76 (s, 3H), 3.71–3.65 (m, 2H), 3.62 (s, 3H), 2.25 (s, 3H), 2.03 (t, J = 7.2 Hz, 2H), 1.60 (dt, J = 14.9, 7.3 Hz, 2H), 1.32–1.18 (m, 4H). ^{13}C NMR (101 MHz, CD_3OD) δ 173.2, 171.5, 153.9, 138.4, 134.9, 131.8, 128.1, 126.3, 125.3, 120.6, 110.1, 109.3, 100.0, 54.8, 50.9, 49.9, 45.7, 31.7, 29.9, 29.7, 25.4, 24.5, 8.9. HRMS (ESI) $[M+H]^+$ calculated for $[C_{28}H_{34}O_5N_5]^+$ was 520.2554, found 520.2543.

*4.1.18. Methyl 2-(1-(4-(1-(7-(hydroxyamino)-7-oxoheptyl)-1H-1,2,3-triazol-4-yl)benzyl)-5-methoxy-2-methyl-1H-indol-3-yl)acetate (**17b**)*

Trityl deprotection of methyl 2-(5-methoxy-2-methyl-1-(4-(1-(7-oxo-7-((trityloxy)amino)heptyl)-1H-1,2,3-triazol-4-yl)benzyl)-1H-indol-3-yl)acetate (0.074 g, 0.095 mmol), an intermediate obtained during the synthesis of **16** above, was achieved as described for **11a**. Purification was done by prep TLC using 10:1 DCM:MeOH to give **17b** as a brown solid (0.025 g, 49%). HPLC retention time 8.48 min. ^{1}H NMR (500 MHz, CD_3OD) δ 8.24 (s, 1H), 7.69 (d, J = 8.0 Hz, 2H), 7.14 (d, J = 8.8 Hz, 1H), 7.04–6.98 (m, 3H), 6.72 (dd, J = 8.8, 2.1 Hz, 1H), 5.36 (s, 2H), 4.40 (t, J = 6.8 Hz, 2H), 3.81 (s, 3H), 3.75 (s, 2H), 3.67 (s, 3H), 2.32 (s, 3H), 2.06 (m, 2H), 1.60 (m, 2H), 1.35 (m, 5H). ^{13}C NMR (126 MHz, CD_3OD) δ 173.4, 171.3, 154.3, 147.3, 138.6, 135.0, 131.8, 129.4, 128.2, 126.3, 125.5, 120.7, 110.3, 109.5, 104.2, 100.2, 55.0, 51.3, 50.0, 45.9, 29.7, 28.9, 28.0, 25.8, 25.1, 9.0. HRMS (ESI) $[M+H]^+$ calculated for $[C_{29}H_{36}O_5N_5]^+$ was 534.2711, found 534.2705.

*4.1.19. Methyl 2-(1-(4-(1-(8-(hydroxyamino)-8-oxooctyl)-1H-1,2,3-triazol-4-yl)benzyl)-5-methoxy-2-methyl-1H-indol-3-yl)acetate (**17c**)*

Reaction of methyl 2-(1-(4-ethynylbenzyl)-5-methoxy-2-methyl-1H-indol-3-yl)acetate (**14**) (0.074 g, 0.21 mmol) with trityl-protected 8-azidooctanehydroxamic acid (0.11 g, 0.26 mmol) in the presence of DIPEA (0.07 mL, 0.43 mmol) and CuI (0.02 g, 0.11 mmol) in THF (10 mL), as described above for **16**, gave methyl 2-(5-methoxy-2-methyl-1-(4-(1-(8-oxo-8-((trityloxy)amino)octyl)-1H-1,2,3-triazol-4-yl)benzyl)-1H-indol-3-yl)acetate (0.026 g, 16%). Trityl deprotection was achieved as described for **11a**. Purification was done by prep TLC using 10:1 DCM:MeOH to give **17c** as a brown solid (0.017 g, 92%). HPLC retention time 9.92 min. ^{1}H NMR (500 MHz, CD_3OD) δ 8.26 (s, 1H), 7.72 (d, J = 7.2 Hz, 2H), 7.16 (d, J = 8.7 Hz, 1H), 7.04 (s, 3H), 6.74 (d, J = 8.6 Hz, 1H), 5.38 (s, 2H), 4.42 (s, 2H), 3.83 (s, 3H), 3.77 (s, 2H), 3.69 (s, 3H), 2.34 (s, 4H), 1.95 (s, 2H), 1.61 (s, 2H), 1.34 (ms, J = 24.6 Hz, 8H). ^{13}C NMR (126 MHz, CD_3OD) δ 175.3, 170.3, 156.4, 149.2, 140.7, 137.1, 133.8, 131.5, 130.3, 128.4, 127.5, 122.8, 112.4, 111.6, 106.2, 102.3, 57.1, 53.1, 52.1, 48.0, 31.8, 30.8, 30.3, 28.1, 27.4, 24.7, 11.1. HRMS (ESI) $[M+H]^+$ calculated for $[C_{30}H_{38}O_5N_5]^+$ was 548.2867, found 548.2855.

4.2. Cell viability assay

All cell lines used in this study (Du-145, LNCaP, HCT-116, A549, MCF-7 and Vero) were maintained in the respective media recommended by ATCC. All the media used were supplemented with 10% fetal bovine serum (FBS) (Atlanta Biologicals, Atlanta, GA) and 1% *Pen. Strep*. Prior to treatment with various drug concentrations and subsequent incubation for 72 h, cells were incubated in a 96 well plate for 24 h. Cell viability was measured using the MTS assay protocol as described by the manufacturer. For all drugs tested, DMSO concentration was maintained at 0.1% for experiments in LNCaP, HCT-116 and DU-145; and at 1% for experiments in other

cell lines. Data was analyzed using the LOGIT function. GRAPHPAD prism software was used to generate all growth-inhibition curves.

4.3. Cell cycle analysis

LNCaP cells were seeded onto 6-well plates at a density of 1×10^6 cells in 5 mL of media, and incubated in a humidified 5% CO_2 atmosphere at 37 °C overnight. Following aspiration of media, fresh media containing drugs were added to the cells and incubated for 24 h. After incubation, cells were trypsinized, harvested and fixed with 70% EtOH. Fixed cells were stained with freshly prepared PI solution containing RNAse A, and then analyzed on flow cytometer (BD FACS Acuri, BD Bioscience, San Jose, CA, USA). Unstained cells were used as control. Each experiment was performed in triplicate.

4.4. Western blots analysis

LNCaP cells (10^6 cells/dish) were seeded in petri dishes 24 h prior to treatment with various concentrations of compounds for 24 h. Thereafter, media was removed and cells were washed with chilled 1× PBS buffer and resuspended in CelLyticM buffer containing a cocktail of protease inhibitor (Sigma-Aldrich, St. Louis, MO, USA). Protein concentration was determined through Bradford protein assay. Equal amount of protein was then loaded onto an SDS-page gel (Bio-Rad, Hercules, CA, USA) and resolved by electrophoresis at a constant voltage of 100 V for 2 h. The gel was transferred onto a nitrocellulose membrane and probed for acetylated tubulin, acetyl H4, AR, COX-2 and actin as loading control.

4.5. HDAC inhibition

The HDAC activity in presence of our compounds was assessed using the SAMDI mass spectrometry. As a label-free technique, SAMDI is compatible with a broad range of native peptide substrates without requiring potentially disruptive fluorophores. To obtain IC_{50} values, we incubated isoform-optimized substrates (20 μM for HDACs 1–2, 6 and 50 μM for HDAC 8) with enzyme (70 nM (HDAC 1), 100 nM (HDAC 2), 50 nM (HDAC 3), 60 nM (HDAC 6), 500 nM (HDAC 8)) and inhibitor (at concentrations ranging from 10 nM to 1.0 mM) in 96-well microtiter plates at 30 °C (24 h (HDAC 1), 24 h (HDAC 2), 5 h (HDAC 3), 20 h (HDAC 6), 2.5 h (HDAC 8)). Solution-phase deacetylation reactions were quenched with trichostatin A (TSA) and transferred to SAMDI plates to immobilize the substrate components. SAMDI plates were composed of an array of self-assembled monolayers (SAMs) presenting maleimide in standard 384-well format for high-throughput handling capability. Following immobilization, plates were washed to remove buffer constituents, enzyme, inhibitor, and any unbound substrate and analyzed by MALDI mass spectrometry using automated protocols.[44] Deacetylation yields in each triplicate sample were determined from the integrated peak intensities of the molecular ions for the substrate and the deacetylated product ion by taking the ratio of the former over the sum of both. Yields were plotted with respect to inhibitor concentration and fitted to obtain IC_{50} values for each isoform-inhibitor pair.

4.6. COX inhibition assay

In vitro COX inhibitory activity was evaluated using Cayman's COX Fluorescent Inhibitor Screening Assay Kit (Cayman Chemical Company, Ann Arbor, MI, USA) following the manufacturer's protocol. Briefly, ovine COX-1 and human recombinant COX-2 enzymes were incubated with stock solutions of our compounds and heme for 15 min at room temperature, after which a resorufin precursor was added and incubated for another 15 min at room temperature. The reaction was started by the adding arachidonic acid and left to proceed for 2 min. Fluorescence was measured at a 530 nm excitation wavelength and a 595 nm emission wavelength using a micro plate reader (Envision, PerkinElmer). Data was analyzed using the LOGIT function.

4.7. Molecular docking analysis

In silico docking was performed using Autodock Vina[45] run through PyRx to manage the workflow and PyMol to visualize the results, as described previously.[19d] Briefly, ligands were prepared by first generating an energy minimized 3D structure in ChemBioDraw3D. This was followed by processing with Autodock Tools 1.5.4. Docking runs were performed within a 25–30 Å cubic search space surrounding the binding pocket.

4.8. Intracellular PGE_2 measurement

HeLa cells (3×10^5 cells/dish) were seeded in 6-well plates 24 h prior to treatment with various concentrations of tested compounds. After incubation for 24 h, the cell culture media was taken and centrifuged at 14,000*g* for 10 min, to remove cellular debris. PGE_2 concentration was determined by using PGE_2 ELISA Kit-monoclonal (catalog number 514010). The assay was performed as recommended by the manufacturer. Briefly, serial dilution of PGE_2 standard and 50 μL of each sample were added to the recommended amount PGE_2 antiserum and acetylcholinesterase tracer and incubated at 4 °C for 18 h. The wells were emptied and washed five times with wash buffer. Thereafter, 200 μL of Ellman's reagent containing substrate for acetylcholinesterase was added. The reaction was developed at room temperature for 2 h on a slow shaker. Plates was read at 405 nm on a micro plate reader (Envision, PerkinElmer). Data was analyzed using the LOGIT function. GRAPHPAD prism software was used to generate graph and perform statistical analyses. Individual runs were normalized with respect to the control, and PGE_2 suppression expressed in terms of percentage.

4.9. Anti-inflammatory activity assay

NF-κB activity was measured using luciferase assay. BEAS-2B cells were transfected with NF-κB luciferase reporter construct in pGL3 basic vector.[46] Forty hours after transfection, the cells were treated with test compounds for 1 h followed by stimulation with NTHi for 5 h. The cells were then lysed with cell lysis buffer (250 mM Tris-HCl (pH 7.5), 0.1% Triton-X, 1 mM DTT) and luciferase activity was measured by using luciferase assay system (Promega). Relative luciferase activity (RLA) was determined using the following equation: RLA = luciferase unit of the cells treated with NTHi and inhibitors/luciferase unit of the cells treated with mock.

Acknowledgement

This project was financially supported by NIH grants R01CA131217 (A.K.O.) and R21CA185690 (A.K.O.) and RO1DC005843 (J.D.L.). Emily Janeira was supported by the Research Experience for Undergraduates (REU) program (summer 2014) at Georgia Institute of Technology. J.D. Li is a Georgia Research Alliance Eminent Scholar in Inflammation and Immunity.

A. Supplementary material

Supplementary data associated with this article can be found, in the online version, at http://dx.doi.org/10.1016/j.bmc.2016.12.032.

References

1. (a) Bowman GD, Poirier MG. *Chem Rev*. 2014;115:2274;
   (b) Minucci S, Pelicci PG. *Nat Rev Cancer*. 2006;6:38.
2. West AC, Johnstone RW. *J Clin Invest*. 2014;124:30.
3. (a) Gryder BE, Sodji QH, Oyelere AK. *Future Med Chem*. 2012;4:505;
   (b) Zhang L, Han Y, Jiang Q, et al. *Med Res Rev*. 2015;35:63.
4. Weichert W. *Cancer Lett*. 2009;280:168.
5. Ratner M. *Nat Biotechnol*. 2014;32:853.
6. Shah MH, Binkley P, Chan K, et al. *Clin Cancer Res*. 2006;12:3997.
7. (a) Tondera C, Ullm S, Laube M, et al. *Biochem Biophys Res Commun*. 2015;458:40;
   (b) Toomey DP, Murphy JF, Conlon KC. *Surgeon*. 2009;7:174.
8. Smith WL, Garavito RM, DeWitt DL. *J Biol Chem*. 1996;271:33157.
9. Yuan C, Smith WLA. *J Biol Chem*. 2014;290:5606.
10. Funk CD. *Science*. 2001;294:1971.
11. Fischer SM, Hawk ET, Lubet RA. *Cancer Prevent Res*. 2011;4:1728.
12. Pan Y, Zhang J-S, Gazi MH, Young CYF. *Cancer Epidemiol Biomark Prev*. 2003;12:769.
13. (a) Kashiwagi E, Shiota M, Yokomizo A, Inokuchi J, Uchiumi T, Naito S. *Prostate Cancer Prostatic Dis*. 2014;17:10;
   (b) Kashiwagi E, Shiota M, Yokomizo A, et al. *Endocr Relat Cancer*. 2013;20:431.
14. Jendrossek V. *Cancer Lett*. 2013;332:313.
15. Li N, Xi Y, Tinsley HN, et al. *Mol Cancer Ther*. 2013;12:1848.
16. Patel MI, Subbaramaiah K, Du B, et al. *Clin Cancer Res*. 2005;11:1999.
17. Masferrer JL, Leahy KM, Koki AT, et al. *Cancer Res*. 2000;60:1306.
18. (a) Zhang H, Fan J, Wang J, Zhang S, Dou B, Peng X. *J Am Chem Soc*. 2013;135:11663;
   (b) Zhang H, Fan J, Wang J, et al. *J Am Chem Soc*. 2013;135:17469;
   (c) Uddin MJ, Crews BC, Ghebreselasie K, et al. *J Biomed Opt*. 2015;20:50502.
19. (a) Musso L, Dallavalle S, Zunino F. *Biochem Pharmacol*. 2015;96:297;
   (b) Guerrant W, Patil V, Canzoneri JC, Oyelere AK. *J Med Chem*. 2012;55:1465;
   (c) Gryder BE, Akbashev MJ, Rood MK, et al. *ACS Chem Biol*. 2013;8:2550;
   (d) Gryder BE, Rood MK, Johnson KA, et al. *J Med Chem*. 2013;56:5782.
20. (a) Neumann W, Crews BC, Sarosi MB, et al. *ChemMedChem*. 2015;10:183;
   (b) Zhang G, Panigrahy D, Hwang SH, et al. *Proc Natl Acad Sci*. 2014;111:11127.
21. Wang X, Li G, Wang A, Zhang Z, Merchan JR, Halmos B. *Mol Carcinog*. 2013;52:218.
22. (a) Uddin MJ, Crews BC, Ghebreselasie K, Tantawy MN, Marnett LJ. *ACS Med Chem Lett*. 2010;2:160;
   (b) Bhardwaj A, Kaur J, Wuest F, Knaus EE. *ChemMedChem*. 2014;9:109;
   (c) Wilson AJ, Chueh AC, Tögel L, et al. *Cancer Res*. 2010;70:609.
23. Uddin MJ, Crews BC, Ghebreselasie K, Marnett LJ. *Bioconjug Chem*. 2013;24:712.
24. Mwakwari SC, Guerrant W, Patil V, et al. *J Med Chem*. 2010;53:6100.
25. Szabó G, Fischer J, Kis-Varga Á, Gyires K. *J Med Chem*. 2007;51:142.
26. Rogez-Florent T, Meignan S, Foulon C, et al. *Bioorg Med Chem*. 2013;21:1451.
27. Dwivedi AK, Gurjar V, Kumar S, Singh N. *Drug Discov Today*. 2015;20:863.
28. Bhardwaj A, Kaur J, Sharma SK, Huang Z, Wuest F, Knaus EE. *Bioorg Med Chem Lett*. 2013;23:163.
29. Liedtke AJ, Adeniji AO, Chen M, et al. *J Med Chem*. 2013;56:2429.
30. Gadgeel SM. *Cancer*. 2015;121:3197.
31. Tang G, Wong JC, Zhang W, et al. *J Med Chem*. 2014;57:8026.
32. Yamaguchi K, Lantowski A, Dannenberg AJ, Subbaramaiah K. *J Biol Chem*. 2005;280:32569.
33. Agarwal B, Swaroop P, Protiva P, Raj SV, Shirin H, Holt PR. *Apoptosis*. 2003;8:649.
34. Feldman BJ, Feldman D. *Nat Rev Cancer*. 2001;1:34.
35. Marrocco DL, Tilley WD, Bianco-Miotto T, et al. *Mol Cancer Ther*. 2007;6:51.
36. Lu X-Y, Wang Z-C, Ren S-Z, Shen F-Q, Man R-J, Zhu H-L. *Bioorg Med Chem Lett*. 2016;26:3491.
37. Lawrence T. *Cold Spring Harb Perspect Biol*. 2009;1:a001651.
38. Tapadar S, Fathi S, Raji I, et al. *Bioorg Med Chem*. 2015;23:7543.
39. (a) Takada Y, Bhardwaj A, Potdar P, Aggarwal BB. *Oncogene*. 2004;23:9247;
   (b) Tegeder I, Pfeilschifter J, Geisslinger G. *FASEB J*. 2001;15:2057.
40. Schroeder FA, Lewis MC, Fass DM, et al. *PLoS ONE*. 2013;8:e71323.
41. (a) Daniel KB, Sullivan ED, Chen Y, et al. *J Med Chem*. 2015;58:4812;
   (b) Ueki N, Lee S, Sampson NS, Hayman MJ. *Nat Commun*. 2013;4:2735.
42. Uddin MJ, Crews BC, Blobaum AL, et al. *Cancer Res*. 2010;70:3618.
43. (a) Sodji QH, Kornacki JR, McDonald JF, Mrksich M, Oyelere AK. *Eur J Med Chem*. 2015;96:340;
   (b) Oyelere AK, Chen PC, Guerrant W, et al. *J Med Chem*. 2008;52:456.
44. Gurard-Levin ZA, Scholle MD, Eisenberg AH, Mrksich M. *ACS Combin Sci*. 2011;13:347.
45. Trott O, Olson AJ. *J Comput Chem*. 2010;31:455.
46. (a) Miyata M, Lee J-Y, Susuki-Miyata S, et al. *Nat Commun*. 2015;6:6062;
   (b) Ishinaga H, Jono H, Lim JH, et al. *EMBO J*. 2007;26:1150.